

211-23  
N77-18092

STATUS OF RUNWAY SLIPPERINESS RESEARCH

Walter B. Horne  
NASA Langley Research Center

SUMMARY

Runway slipperiness research performed in the United States and Europe since 1968 has been reviewed. This review suggests the following benefits to the aviation community: Better understanding of the hydroplaning phenomena; a method for predicting aircraft tire performance on wet runways from a ground-vehicle braking test; runway rubber deposits identified serious threat to aircraft operational safety; methods developed for removing rubber deposits and restoring runway traction to uncontaminated surface levels; and developed antihydroplaning runway surfaces, such as pavement grooving and porous friction course, which considerably reduce the possibility of encountering aircraft hydroplaning during landings in rainstorms.

INTRODUCTION

Extensive research has been performed in the United States and Europe since 1968 in an effort to combat problems relative to aircraft operations on slippery runways. This research has led to a more complete understanding of the sources of these operating problems and, as a result, improved methods are being introduced to control or alleviate these problems. The purpose of this paper is to review the present status of runway slipperiness research in the following areas of interest:

- (1) Runway flooding during rainstorms
- (2) Hydroplaning
- (3) Identification of slippery runways including the results from ground vehicle friction measurements and attempts to correlate these measurements with aircraft stopping performance
- (4) Progress and problems associated with the development of antihydroplaning runway surface treatments such as pavement grooving and porous friction course (PFC)
- (5) Runway rubber deposits and their removal

## RUNWAY FLOODING DURING RAINSTORMS

During 1971, the Texas Transportation Institute (TTI), Texas A&M University, published the results of a comprehensive study on the effects of rainfall intensity, pavement cross slope, surface texture, and drainage length on pavement water depths (ref. 1). From the TTI study, an equation can be derived to predict the rainfall intensity required to initiate flooding in aircraft tire paths on the runway as follows:

For SI Units:

$$I_F = 1.253 \times 10^3 \left[ \frac{T^{.89}}{L^{.43} (1/S)^{.42}} \right]^{1.695} \quad (1a)$$

For U.S. Customary Units:

$$I_F = 1.543 \times 10^4 \left[ \frac{T^{.89}}{L^{.43} (1/S)^{.42}} \right]^{1.695} \quad (1b)$$

where

- $I_F$  rain rate required to initiate runway flooding in tire path, mm/hr (in/hr)
- $T$  pavement surface texture depth (ATD), mm (in.)
- $L$  tire path distance from runway crown, m (ft)
- $S$  runway cross slope, m/m (ft/ft)

It should be noted that equations (1) are derived from data obtained on ungrooved pavements and from pavements that have not been treated with a porous friction course. Figure 1 illustrates how equations (1) can be used to predict whether a flooded runway condition will exist for a typical jet transport landing on the runway center line during a rainstorm. The trends shown in figure 1 suggest that a pavement must be provided with a good cross slope and a good surface texture to minimize the risk of runway flooding and dynamic hydroplaning occurring to aircraft during take-off and landing in rainstorms.

### Effect of Surface Winds on Drainage

Surface winds, when present on runways, can appreciably affect runway drainage by changing the direction of water flow off the side of the runway which tends to increase the drainage path length and increase runway water depths. Observations of water drainage from a number of runways using a dye test (sodium

fluorescein dye injected into draining water on the runway to improve flow visualization) suggest that surface winds do not appreciably affect water drainage from runways as long as the draining water is flowing below the top of the pavement texture. Surface winds do affect water drainage from runways when flooded conditions exist and the water is flowing as a sheet above the top of the pavement texture. In the latter case, the water drainage-path angle with respect to the runway center line is determined from the vector sum of the wind and gravitational forces acting on the water. Typical examples of this behavior are shown in figure 2 (ref. 2) where the water drainage patterns (from a dye test) obtained on a conventional burlap drag and a wire-combed (plastic grooved) concrete runway surfaces during artificial wetting tests performed in a 10-knot surface wind are compared. The average texture depth (ATD) of the ungrooved burlap drag surface was 0.28 mm (0.011 in.) as measured by the NASA grease test. This texture depth was insufficient to prevent surface flooding under the artificial wetting conditions, and the water drainage path direction was rotated toward the runway center line by the action of the surface wind. Under the same surface wetting and wind condition, the grooved concrete surface with an ATD of 0.81 mm (0.032 in.) allowed most of the draining water to flow below the top of the surface texture (unaffected by wind). As a consequence, the water drainage path on this surface was nearly inline with the transverse grooves and the runway cross slope.

#### Flooding on Grooved Runways

NASA has constructed a concrete runway 4372 m (15 000 ft) long and 91 m (300 ft) wide at the Kennedy Space Center (KSC) for the space shuttle. (See fig. 3.) A longitudinal broom surfacing treatment was given the fresh concrete as it was paved by a slip-form paver (fig. 4). The concrete runway surface several months after paving was grooved by diamond saws to a transverse  $29 \times 6 \times 6$  mm ( $1\frac{1}{8} \times \frac{1}{4} \times \frac{1}{4}$  in.) pattern with the resulting surface texture shown in figures 5 and 6. The Langley Research Center (LaRC) performed drainage and traction studies on the space shuttle runway in June 1976.

On June 20, 1976, the Cape Canaveral area was subjected to a series of thunderstorms during which heavy rain fell on the shuttle runway. Figure 7 shows the rain rates and surface flooding that occurred on the shuttle runway during a 30-minute period as one of the thunderstorms passed over the runway. The space shuttle runway is oriented in a north/south direction; a wind of approximately 10 knots magnitude from the southwest was observed during the storm. For this wind condition, the data in figure 7 show that a rain rate of approximately 81 mm/hr (3.2 in/hr) is required to start runway flooding in the shuttle main gear tire paths (landing on runway center line).

The predicted rain rate (from eqs. (1)) required to flood the runway in the shuttle main tire path is 47.1 mm/hr (1.85 in/hr). This difference between observed (81 mm/hr (3.2 in/hr)) and estimated (47.1 mm/hr (1.85 in/hr)) rain rates gives added weight to features long observed on runways grooved with a diamond saw technique; that is, the polished groove channels (from the diamond saw cuts) greatly reduce water flow resistance over water draining through and over the comparatively much rougher texture of conventional surface treatments.

In addition, the draining water is forced by the groove channels to take the shortest drainage path (down the grooves) off the runway edge even on runways with longitudinal slope. As a consequence, water drainage from runways grooved with the diamond saw technique is greatly increased over ungrooved runway surfaces. (See fig. 8.) It is believed that plastic grooving techniques are not as effective as the sawed groove technique for water drainage because the grooves can be interrupted or misaligned at paving lane edges and the groove channels have rougher wall surfaces.

#### Flooding on Porous Friction Course Runways

Water drainage from the porous friction course (PFC) runway at Farnborough, England, was personally observed during a heavy rain in 1965 and the runway did not flood while adjacent conventional surfaces did. Most PFC surfaces are 19 mm (3/4 in.) thick and have void ratios ranging between 0.1 and 0.15, which give this surface treatment a high water storage capacity before the surface floods. However, water drainage over and through this surface treatment is interstitial with many abrupt flow direction changes as well as rough flow surfaces. Consequently, the drainage-path lengths will be longer for a PFC surface than for a grooved surface, especially on runways with longitudinal slope. For these reasons, it is believed, but not yet substantiated, that PFC surfaces will not drain water from runways as effectively as grooved surfaces (diamond saws) during prolonged rainfalls having high rainfall rates.

#### HYDROPLANING

The three presently known types of hydroplaning were first defined in reference 2, that is, dynamic, viscous, and "reverted" rubber hydroplaning. Continuing research on hydroplaning since that time has in general supported the conclusions reached in reference 2. However, this later research has shown new aspects of hydroplaning that are significant and of importance to describe.

#### Wheel Spin-Up Speed

Early (1960) NASA track hydroplaning research was conducted by rolling full-size unbraked aircraft tires across dry and flooded runway sections. The aircraft tire spun up at touchdown on the dry pavement and then entered the flooded runway section at synchronous runway wheel speed and subsequently spun down or stopped completely when the carriage speed equaled or exceeded the tire hydroplaning speed. This type of test defined the well-known tire hydroplaning speed equation (ref. 3), which is given as follows:

For SI Units:

$$(V_p)_{\text{spin-down}} \approx 3.43 \sqrt{p} \quad (2a)$$

For U.S. Customary Units:

$$(V_P)_{\text{spin-down}} \approx 9 \sqrt{p} \quad (2b)$$

where

$(V_P)_{\text{spin-down}}$  tire spin-down hydroplaning speed, knots

$p$  tire inflation pressure, kPa (lb/in<sup>2</sup>)

Since 1960, the aircraft industry has used this equation to define the hydroplaning speed for particular aircraft and aircraft flight manuals. Starting in 1970, investigation of aircraft hydroplaning accidents suggested that the spin-up hydroplaning speed for a nonrotating aircraft tire (as at aircraft touchdown) might be lower in magnitude than the speed predicted by equations (2) for a rolling unbraked tire. (See refs. 4 and 5.) As a consequence, references 6 and 7 defined the tire wheel spin-up hydroplaning speed on flooded runways as

For SI Units:

$$(V_P)_{\text{spin-up}} \approx 2.93 \sqrt{p} \quad (3a)$$

For U.S. Customary Units:

$$(V_P)_{\text{spin-up}} \approx 7.7 \sqrt{p} \quad (3b)$$

where

$(V_P)_{\text{spin-up}}$  tire spin-up hydroplaning speed, knots

$p$  tire inflation pressure, kPa (lb/in<sup>2</sup>)

Additional verification of this new hydroplaning equation (eqs. (3)) is given in reference 8 and shown in figure 9. It is important that aircraft flight-manual hydroplaning speeds be changed to reflect the values given by equations (3) since this hydroplaning speed represents the actual tire situation for aircraft touchdown on flooded runways.

#### Reverted Rubber Hydroplaning

Reverted rubber hydroplaning was first recognized and defined from friction data produced at the Langley landing-loads track (ref. 2), now called the

Langley aircraft landing loads and traction facility, and from investigation of NTSB (National Transportation Safety Board) aircraft skidding accident reports prior to 1965. (Data from the Langley landing-loads track or the Langley aircraft landing loads and traction facility are herein after designated "NASA track data," and the facility is designated "NASA track.") Full-scale aircraft verification of the extremely low friction values encountered during reverted rubber hydroplaning did not occur until the aircraft flight test programs that are reported in references 9 to 11. These flight test programs were conducted in 1971-73. Figure 10 shows the reverted rubber skid patch developed on a B-737 tire during a landing run on the artificially wet runway at Roswell, New Mexico, after an approximately 1829-m (6000-ft) slide-out with all four main gear tires of the B-737 in a locked-wheel condition. Figure 11 shows the comparison between the Langley friction results of 1965 and the B-727 (1971) and the B-737 (1973) full-scale braking tests. The aircraft friction data shown in this figure completely validate the 1965 NASA track data and confirm the belief that the reverted rubber skid mode is the most catastrophic for aircraft operational safety because of the low braking friction and the additional fact that tire cornering capability drops to zero when wheels are locked. (See ref. 8.)

The reverted rubber hydroplaning condition is limited to aircraft using high tire inflation pressures. This phenomenon has not been observed on ground vehicles employing low tire inflation pressures of 165 kPa (24 lb/in<sup>2</sup>) or less when vehicle wheels are locked. Reverted rubber hydroplaning develops only when prolonged wheel lockups occur which stem from pilot/antiskid braking system inputs. Thus, the avoidance of reverted rubber hydroplaning must rest with improving pilot braking procedures and with improving locked-wheel protection circuits of aircraft antiskid braking systems. (See ref. 8.)

#### Combined Viscous and Dynamic Hydroplaning

Most researchers now agree that the loss of tire friction on wet or flooded pavements with speed is due to the combined effects of viscous and dynamic hydroplaning phenomena acting in the tire footprint as shown in figure 12. The tire hydroplaning model shown in this figure was first proposed by Gough in 1959 in reference 12. (See also ref. 13.) The footprint and sketch in this figure show a pneumatic rolling at medium speed across a flooded pavement. For this partial hydroplaning condition, zone 1 describes the fraction of the tire footprint that is supported by bulk water, zone 2 describes the fraction of tire footprint that is supported by a thin water film, and zone 3 describes the fraction of the tire footprint that is in essentially dry contact with the peaks of the pavement surface texture. The length of zone 1 represents the time required for the rolling tire for this speed condition to expel bulk water from under the footprint; correspondingly, the length of zone 2 represents the time required for the tire to squeeze out the residual thin water film remaining under the footprint after the bulk water has been removed. Since fluids cannot develop shear forces of appreciable magnitude, it is only in zone 3 (essentially dry region) that traction forces for steering, decelerating, and accelerating a vehicle can be developed between the tire and the pavement. The ratio of the

dry contact area (zone 3) to the total tire footprint area (zone 1 + zone 2 + zone 3) multiplied by the friction coefficient the tire develops on a dry pavement yields the friction coefficient the tire can develop for this flooded pavement and speed condition.

As speed is increased, a point is reached where zone 3 disappears and the entire footprint is supported by either bulk water or a thin water film. This speed condition is called combined viscous and dynamic hydroplaning. As speed is further increased a point is reached where bulk water penetrates the entire tire footprint. This condition is called dynamic hydroplaning. If the runway is not flooded (no bulk water) such as on a runway covered with a heavy dew, it is possible for zone 2 to cover the entire tire footprint at speed if the pavement is very smooth. This condition is called viscous hydroplaning.

#### Water Pressure Propagation Under the Tire Footprint

NASA track research (ref. 2) shows that the fluid pressure developed in the bulk water (zone 1) region of the footprint follows a  $V^2$  law and stems from fluid inertial or density properties as shown in figure 12. Correspondingly, this research shows that the fluid pressure developed in zone 2 (fig. 12) stems from fluid viscous properties; hence, the names dynamic and viscous hydroplaning are used to describe the hydroplaning phenomena.

#### Pavement Macro/Microtexture Effects on Hydroplaning

When flooding on a runway occurs, the pavement surface macrotexture plays the important role of providing escape channels to drain bulk water from zone 1 (fig. 12). The drainage channels are provided by the tire tread draping over the high spots (asperities) of the pavement surface texture leaving valleys between the tire tread and the low points of the surface texture through which bulk water can easily drain out from under the tire footprint. Bulk water drainage through the pavement macrotexture thus delays to much higher speeds the buildup of fluid dynamic pressure with speed found for pavements with no or poor macrotexture. This effect is illustrated in figure 12 for smooth and grooved pavements. The macrotexture of a pavement can be assessed to some degree by methods such as the NASA grease test (ref. 14), the British sand patch test (ref. 15), and the Texas Transportation Institute silicone putty test (ref. 16).

Providing the pavement with a good microtexture is the major means of combating viscous hydroplaning or preventing the development of viscous fluid pressures in zone 2 of the tire footprint. (See fig. 12.) Pavement microtexture is difficult to detect by eye but can usually be determined from touching the surface. A good pavement microtexture has a sharp-harsh-gritty feel such as obtained when touching fine sandpaper. The touch test is qualitative and not infallible and should be confirmed by ground vehicle friction tests under wet conditions. Pavement microtexture performs its function by providing the pavement surface thousands of sharp pointed projections that, when contacted by the tire tread, generate local bearing pressures of several thousand Pa ( $1\text{b}/\text{in}^2$ ).

This intense pressure quickly breaks down the thin water film coating the pavement surface, and allows the tire to regain dry contact with the high points of the pavement surface texture.

### Tire Effects on Hydroplaning

The footprint of the tire can be considered analogous to the wing on an aircraft; both are lifting surfaces, the wing to support the weight of the aircraft in flight through the atmosphere and the tire footprint to support the weight of the vehicle during hydroplaning on a wet or flooded pavement. Wings of high aspect ratio (wing length/chord length) reduce tip losses and produce the highest lift coefficient to support the aircraft in flight. Research shows the same trends for tire footprints. Smooth tread tires having high-aspect-ratio footprints (footprint width/footprint length) for similar conditions of flooded pavement, load, and inflation pressure will hydroplane at lower vehicle speeds than tires with low-aspect-ratio footprints. The aspect ratio of the tire footprint is governed by the shape of the tire cross section or the ratio of tire section height to section width (also called the tire aspect ratio).

Molding grooves (channels) in the tire tread at time of construction is the tire designers equivalent of pavement macrotexture. The tread grooves in the tire footprint are vented to atmosphere and provide escape channels for the bulk water trapped in zone 1 (fig. 12). Tread grooves thus raise the critical water depth required for a tire to suffer dynamic hydroplaning, and for water depths less than the critical depth, raise the tire hydroplaning speed. It should be noted that the benefits from grooving the tire tread decrease in proportion to tread wear (depth of groove) and vanish when the groove depth decreases to 1.6 mm (1/16 in.) or less. The tire designers equivalent of pavement microtexture is to cut or mold kerfs or sipes into the tread ribs that lie between the tread grooves. The purpose of these features is to greatly increase the number of sharp edges of tread contact with the pavement that are provided by the tread grooves. Contact of the pavement surface at these sharp cornered tread sipe and groove edges creates local bearing pressures sufficiently high to quickly breakdown and displace the thin water film (zone 2, fig. 12) that creates viscous hydroplaning.

The vertical load acting on a tire divided by the tire footprint area determines the average tire-pavement contact pressure. For smooth tread tires, this contact pressure is approximately equal or proportional to the tire inflation pressure. The difference in the pressure within and without (atmospheric pressure) the tire footprint creates forces which expel the water trapped in the tire-pavement contact zone at velocities which are proportional to the square root of the tire tread-pavement contact pressures. Thus, increasing the inflation pressure in a tire increases the rate of flow of water drainage out of the footprint and raises the tire hydroplaning speed. When grooves are cut or molded into a tire tread to form a tread pattern, the area of actual rubber contact with the pavement in the tire footprint is reduced. The result is that the contact pressures on the ribs of the tread pattern are increased which increases the rate of flow of water draining out of the footprint. This fact explains the effectiveness of tire tread patterns in improving wet traction or

delaying hydroplaning effects on wet or flooded pavements to higher speeds. It should be noted that while tire tread designs can reduce wet runway traction losses, the improvements obtained are relatively small in comparison to what can be obtained by providing the pavement with a good micro/macrotecture (ref. 7), and these improvements disappear when the tread becomes worn.

#### Tire Operating Mode Effects on Hydroplaning

The tire operating mode is controlled by the vehicle operator (pilot or driver). Depending upon the maneuver required, the vehicle tires may be undergoing free rolling, braked rolling, yawed rolling, powered rolling, a combination of braked and yawed rolling, or a combination of powered and yawed rolling. Maximum lateral or steering forces for the tire occur when the tire is neither braked nor powered (driven by the engine). Correspondingly, maximum traction for accelerating or decelerating the vehicle develops when the vehicle is moving straight ahead (unyawed) and the tires are not developing lateral forces to withstand a cross wind or to conduct a turning maneuver. If the driver applies power to the vehicle driving wheels in excess of the tire-pavement friction capability, the tire loses its grip on the pavement, and the wheel will start to spin up with respect to the pavement. The resulting relative motion between the tire and the pavement under wet conditions increases viscous-dynamic hydroplaning effects and traction for accelerating and steering the vehicle is greatly reduced. On the other hand, if the pilot or driver braking demand (brake application) exceeds the tire-pavement friction capability, the tire loses its grip with the pavement and rapidly spins down to a locked-wheel condition. This is the most hazardous tire operating mode for vehicle operational safety (refs. 7, 8, and 17) because the tire cornering capability drops to zero even on dry pavements and vehicle directional stability is greatly reduced. Research shows that on wet and flooded pavements, both viscous and dynamic fluid pressures increase in magnitude under the sliding tire footprint over those obtained for a rolling tire for the same speed condition. The result is that locked-wheel sliding or nonrotating tires have a lower hydroplaning speed than rolling tires (compare eqs. (2) and (3)). Under partial hydroplaning conditions on wet runways, the braking traction can be reduced by as much as one-third to two-thirds the maximum obtained during the braked rolling mode from this enhanced hydroplaning effect as shown in figure 11. (Compare  $\mu_{max}$  with  $\mu_{skid}$  for normal rubber.)

#### Prediction of Tire Braking and Cornering Characteristics on Wet Runways

The description of the hydroplaning process given in the preceding paragraphs was taken from the preamble of an empirically derived combined viscous-dynamic hydroplaning theory which is being developed by Horne (LaRC) and Merritt (FAA, Flight Standards). This theory is presently being refined and tested by using NASA track tire data and data obtained from aircraft-ground vehicle runway test programs. The theory was first exposed to public view at the FAA/Industry Meeting on Runway Traction and Rational Landing Rule (Washington, D.C.), February 11-13, 1975. The theory is being used to develop tire-runway friction

models for flight simulator research conducted under NASA Contract (ref. 18), and is being used by NASA to assist NTSB in the investigation of aircraft skidding accidents on wet runways.

One of the first major accomplishments of the theory is the development of a simple method for transforming experimental friction measurements made by a vehicle using one tire operating mode on a wet pavement to prediction of braking and cornering friction coefficients for other tire sizes and different tire operating modes for this same wet pavement condition. The method is described herein with the aid of figures 13 and 14 for the case of a diagonal-braked vehicle (DBV) friction measurement of the wet runway at Roswell, New Mexico, and the corresponding prediction of a B-737 main gear tire friction performance for the same runway wetness condition.

The DBV method for evaluating the slipperiness of wet runways is to lock a diagonal pair of wheels on a four-wheel ground vehicle at a speed of 52.2 knots and decelerate the vehicle to a stop under both wet and dry runway conditions. (See ref. 19.) The wet-dry stopping distance ratio (SDR) obtained is an index to the slipperiness of the runway surface; the higher the SDR, the slipperier the runway is under wet conditions. The upper left plot shown in figure 13 describes the variation of DBV ground speed with time during a typical DBV test run at Roswell during the B-737 flight test program described in references 10 and 11. This speed time history was differentiated with respect to time to obtain the curve for DBV  $\mu_{skid}$  against speed shown in the upper right plot of figure 13. The values of DBV  $\mu_{skid}$  were obtained from the equation

$$DBV \mu_{skid} = 2 \left[ \left( \frac{dv}{dt} \right)_{braked} - \left( \frac{dv}{dt} \right)_{unbraked} \right] \quad (4)$$

The viscous-dynamic hydroplaning theory states that any experimentally obtained variation of tire friction coefficient with speed on a wet pavement can be converted to an equivalent nondimensional hydroplaning-parameter ( $\bar{Y}$ )-speed-ratio form (lower left plot of fig. 13) by means of the relationships

$$\bar{Y} = \frac{\mu_{wet}}{\mu_{dry}} \quad (5)$$

$$Speed \ ratio = \frac{V}{V_p} \quad (6)$$

where

$\mu_{dry}$  characteristic dry friction coefficient for tire

$\mu_{wet}$  experimental or predicted friction coefficient for wet pavement conditions

- $V_G$  ground speed
- $V_P$  characteristic tire hydroplaning speed (obtained from eqs. (2))
- $\bar{Y}$  tire-pavement drainage characteristic or hydroplaning parameter for pavement
- $\bar{Y}_L$   $\bar{Y}$  for locked-wheel sliding (nonrotating tire)
- $\bar{Y}_R$   $\bar{Y}$  for braked or yawed rolling (rotating tire)

The theory defines  $\mu_{dry}$  as the maximum friction coefficient obtainable on a dry pavement under braked rolling, yawed rolling, or locked-wheel sliding conditions at low speed ( $V_G < 2$  knots). For aircraft tires,  $\mu_{dry}$  may be calculated from the following equation (derived from ref. 20):

For SI Units:

$$\mu_{dry} = 0.93 - 1.6 \times 10^{-4} p \quad (7a)$$

For U.S. Customary Units:

$$\mu_{dry} = 0.93 - 1.1 \times 10^{-3} p \quad (7b)$$

where

$p$  tire inflation pressure, kPa (lb/in<sup>2</sup>)

The value of  $\mu_{dry}$  for ground-vehicle tires must be determined experimentally. Typical values of  $\mu_{dry}$  found for ground-vehicle friction measuring devices are listed in table 1. If  $\mu_{dry} = 1.15$  and  $V_P = 44.1$  knots (from eqs. (2)) in equations (5) and (6), respectively, the curve for DBV  $\mu_{skid}$  against  $V_G$  of figure 13 is converted to the curve for  $\bar{Y}_L$  against  $V_G$  shown in the lower left plot of figure 13. The curve of  $\bar{Y}_R$  (rolling tire) shown in this latter plot was obtained with the aid of figure 14 which is empirically derived from NASA track aircraft tire data in the viscous-dynamic hydroplaning theory.

The theory suggests that all experimental pneumatic tire friction coefficients (aircraft or ground vehicle), when converted to nondimensional form, will condense along either the  $\bar{Y}_L$  curve (locked-wheel braking tests) or the  $\bar{Y}_R$  curve (peak-braking or yawed-rolling tests) if the correct values for  $\mu_{dry}$  and  $V_P$  for the tire conditions are used, and the pavement micro/macrotecture and wetness conditions remain constant for the pavement during the tests.

Prediction of friction coefficients for any other tire size and inflation pressure simply requires multiplying either  $\bar{Y}_L$  or  $\bar{Y}_R$  in figure 13 by the

appropriate  $\mu_{dry}$  value for the desired tire condition and the speed ratio  $V_G/V_P$  by the appropriate value of  $V_P$  for the desired tire condition for each data point  $(\bar{Y}, V_G/V_P)$ . For the B-737 tire friction coefficient prediction shown in figure 13,  $\mu_{dry} = 0.75$  and  $V_P = 115.6$  knots were used. These values were predicted by the B-737 test tire inflation pressure of  $p = 1137$  kPa ( $165$  lb/in<sup>2</sup>). Figure 13 shows that the prediction of the theory using DBV test data is within reasonable agreement of the NASA track friction data over the speed range studied for the B-737 tire.

#### IDENTIFICATION OF SLIPPERY RUNWAYS

A main goal of runway slipperiness research has been to find ways to identify slippery runways so that such runways can be remedied and made safe for aircraft adverse weather operation. It has always been realized that it would be very expensive and impractical to utilize specially instrumented aircraft for this purpose; therefore, much research attention has been devoted to developing suitable ground-vehicle friction measuring techniques and equipment for this purpose. Since 1968, extensive aircraft/ground-vehicle runway research programs have been carried out in this country and abroad to find a solution to this problem (refs. 9 to 11, 19, and 21 to 26), and to answer the fundamental questions:

- (1) Do friction measuring devices correlate between themselves?
- (2) Do friction measuring devices correlate with aircraft tire performance on wet runways?
- (3) Do friction measuring devices correlate with aircraft stopping performance on wet runways?

The scope of this aircraft/ground-vehicle correlation problem is indicated by the data trends shown in figures 15 and 16. It can be seen that the data obtained by the various friction measuring devices and two aircraft, all of which utilize different tire operational modes in testing, literally fill the figures, and poor correlation between ground vehicle to ground vehicle, ground vehicle to aircraft, and aircraft to aircraft is indicated. The data in figures 15 and 16 were obtained from references 21, 22, and 27.

#### Ground-Vehicle/Ground-Vehicle Correlation

Ground-vehicle/ground-vehicle correlation is complicated by the fact that the tire sizes, operating modes, and inflation pressures, as well as test speed or test speed ranges, used by the ground-vehicle devices in measuring runway slipperiness are usually significantly different. Historically, most correlation attempts between devices have compared the measurement output of one device against that of another as shown in figures 17 and 18. These figures compare  $1/SDR$  for the DBV against the Mu-Meter friction reading. Both measurements of runway slipperiness were obtained under identical runway wetness conditions on many different runway surfaces tested by USAF (fig. 17 (data

from ref. 28)) and FAA (fig. 18 (data from ref. 29)). The data shown in both figures exhibit similar trends and indicate very poor correlation between a device (DBV) which measures vehicle stopping distance over a speed range of 52.2 to 0 knots with diagonal wheels locked and a yawed-rolling trailer which measures tire cornering force at constant yaw angle ( $\psi = 7.5^\circ$ ) and constant speed ( $V_G = 34.8$  knots) for the wet runway surfaces investigated. A similar trend is noted for the Roswell smooth concrete runway surface shown in figure 19. In this instance only one runway surface was tested, but the runway wetness condition (water depth) varied. These data for the DBV and Mu-Meter were obtained from reference 11. Figures 20 and 21 show the correlation obtained between the DBV and the skiddometer and the DBV and the Miles trailer at Roswell (ref. 11), respectively. The data in these figures show that the skiddometer (fig. 20) (like the Mu-Meter) exhibits poor correlation with DBV SDR measurements, whereas the Miles trailer compares better (fig. 21). The skiddometer runway slipperiness rating was achieved by testing the pavement at a constant speed of 34.8 knots (like the Mu-Meter), whereas the Miles trailer tested the pavement over a speed range of 85 to 0 knots (similar to the DBV).

Much better correlation between ground vehicles is obtained when each vehicle is tested over a speed range and the viscous-hydroplaning theory method (described earlier) is used to compare the friction data obtained by the vehicles. This type of correlation is shown in figures 22 to 25. The data for these figures were obtained from the joint NASA-British Ministry of Technology Skid Correlation Study reported in references 21, 22, and 30. The data trends shown in figures 22 to 25 suggest that good correlation is achieved between ground vehicles when the friction measurement of a vehicle is compared over a speed range with its equivalent measurement from another ground-vehicle device. This result suggests that ground-vehicle runway slipperiness measurements can correlate if tested over a speed range and proper accounting is made for the difference in the tire operating modes between the vehicles. It should be noted that the worst correlation between devices occurs in figure 25 where the Mu-Meter is compared with several other friction measuring devices. The Mu-Meter is the only friction device that does not measure a friction boundary condition - that is, the skiddometer measures peak braking (constant 0.13 braking slip); the General Motors (GM) trailer, either  $\mu_{max}$  or  $\mu_{skid}$  from a pulse braking technique; the Miles trailer,  $\mu_{skid}$  from a pulse braking technique; and the DBV,  $\mu_{skid}$  from a continuous locked-wheel braking technique. The Mu-Meter, on the other hand, measures cornering force developed on a tire at  $7.5^\circ$  yaw angle. At high pavement friction values, it cannot measure the peak friction boundary condition, whereas for low friction conditions, it may measure cornering force after the peak cornering-force value has been obtained, as shown in figure 26. The data in figure 26 were obtained from reference 31 (p. 654). These data suggest that if the yaw angle for maximum cornering force (limiting coefficient of friction) is exceeded, the cornering force (and cornering friction coefficient) is reduced as yaw angle is further increased. For the case of the Mu-Meter which measures cornering force at  $7.5^\circ$  yaw angle, this type of tire behavior may result in an overestimation of the slipperiness of the wet pavement defined by peak boundary friction conditions.

## Aircraft/Ground-Vehicle Correlation

As with ground-vehicle/ground-vehicle correlation attempts, most aircraft/ground-vehicle correlation attempts try to relate the measured output of a friction device with some measured output of the aircraft from data obtained during joint testing of the device and aircraft on artificially wet runway surfaces. Typical aircraft/ground-vehicle relationships obtained from such test programs are shown in figures 27 (Mu-Meter, ref. 24) and 28 (DBV, refs. 11 and 25). Each friction device advocate claims good correlation between the device and the aircraft. For example, reference 26 states that the Mu-Meter may predict aircraft stopping performance within 10 to 15 percent if a correlation ranking system classifying runway surfaces into different texture groups is used. On the other hand, reference 11 states that the DBV can predict aircraft stopping performance within  $\pm 15$  percent by using its prediction method. The tire friction prediction method (described earlier in the paper) offers another approach to show correlation between ground-vehicle and aircraft measurements of runway slipperiness.

Equation (5) may be modified to the form

$$\mu_{\text{eff}} = \eta \bar{Y}_R \mu_{\text{dry}} \quad (8)$$

where

$\mu_{\text{eff}}$  effective braking friction coefficient realized by the aircraft through its antiskid braking system

$\bar{Y}_R$  runway tire-pavement drainage characteristic (hydroplaning parameter) determined by ground-vehicle friction test over ground speed range

$\mu_{\text{dry}}$  characteristic maximum aircraft tire friction coefficient on dry pavement

$\eta$  antiskid braking system efficiency,  $\mu_{\text{eff}}/\mu_{\text{max}}$

This method, using the DBV friction measuring device, is illustrated in figures 29 to 31. The correlation shown in the figures resulted from use of the arbitrarily selected antiskid braking system efficiency model depicted in figure 29 which is patterned after the one described in reference 32.

The data trends shown in figures 29 to 31 suggest that a ground-vehicle friction measuring device can be used to predict the effective friction coefficient an aircraft will develop on a wet runway providing the antiskid braking system efficiency of the aircraft is known. The data trends also suggest that each aircraft type has its own characteristic antiskid braking system efficiency which is dependent upon the landing gear, braking, and antiskid system design.

### Summary of Correlation Results

The runway slipperiness research conducted since 1968 in the area of ground-vehicle/ground-vehicle and aircraft/ground-vehicle correlations has been reviewed and yields the following observations:

Ground-vehicle devices that test at constant speed do not correlate well with those devices that test over a speed range.

Ground-vehicle devices that test at constant speed can be correlated together as well as those that test over a speed range regardless of the tire operating mode during testing.

The DBV can be used to predict aircraft tire braking and cornering characteristics on wet runways. Other ground-vehicle devices have the potential to predict these tire characteristics as well if their test procedure is changed from a constant speed test to a speed range test similar to the DBV. Ground-vehicle devices that test at constant speed cannot predict aircraft tire braking and cornering friction coefficient on wet runways over the full take-off and landing speed range of aircraft.

Ground-vehicle and aircraft slipperiness measurements can be correlated. However, the precision of correlation is obtained from artificially wet runway test programs. The accuracy of prediction from the correlation may be degraded when runways are wet from natural rain (different water depths). Further, some of the older aircraft braking systems can allow locked-wheel operation during maximum braking operation on wet runways. The locked-wheel condition can result in reverted rubber hydroplaning which destroys the aircraft/ground-vehicle correlation. For these reasons, predictions of aircraft braking performance on wet runways from ground-vehicle devices should be employed only to provide guidance information to pilots.

### Status of Runway Slipperiness Measurements

Standard USAF runway skid resistant tests.— Since November 1973, the Air Force Civil Engineering Center (AFCEC) has been measuring the skid resistance properties of airfields. Procedures for conducting the standard skid resistance tests are given in reference 33. This test requires that friction measurements be obtained by both the DBV and Mu-Meter when testing an airfield pavement. AFCEC feels that the friction data obtained from these friction measuring devices are complementary, and together they provide an adequate data base to evaluate the skid resistance of an airfield pavement. AFCEC intends to survey the skid resistance of all USAF runways in the United States and overseas on a periodic basis. AFCEC feels strongly that the concept of using an experienced, well-trained crew and standardized testing procedures for pavement skid resistance evaluations offers many advantages. This concept requires the Air Force to purchase and maintain a minimum quantity of equipment and ensures that the testing is properly accomplished and documented. Results from this Air Force program are reported in references 28 and 34.

FAA Advisory Circular No. 150/5320-12.- FAA Airports Service issued FAA Advisory Circular No. 150/5320-12 on June 30, 1975 (ref. 35). This advisory circular provides guidance on methods that can be used to provide and maintain airport pavement surface friction characteristics. This guidance is intended for use by airport operators, engineering consultants, and maintenance personnel. This advisory circular does not purport to provide a means to predict aircraft stopping distance. For the requirements specified in this circular, FAA Airports Service requires a friction measuring device which

- (1) Can provide fast, accurate, and reliable friction values of airport pavement surfaces under varying climatic conditions
- (2) Can provide a continuous graph record of the pavement surface characteristics
- (3) Has minimal maintenance and recurring costs
- (4) Has a simple calibration technique
- (5) Indicates potential for hydroplaning conditions

This circular is worded carefully such that current friction measuring devices, the DBV for example, are not excluded from use in implementing the circular, although it is clear that the British Mu-Meter is the device favored by FAA Airports Service since it is the only device described in the circular. The advisory circular clearly indicates that its needs are met by a device which measures the relative friction of pavement surfaces and that this measurement of friction does not provide a means to predict aircraft stopping distance (determine how slippery the runway surfaces are for aircraft operation).

It is felt that issuance of this advisory circular by the FAA is a noteworthy step forward in providing guidance to install antihydroplaning runway surfaces at airports. However, the providing of relative friction measurements for engineering and maintenance purposes is secondary to the main objective of a friction evaluation which is to determine how slippery the runway surface is for aircraft operation.

#### PROGRESS AND PROBLEMS OF ANTIHYDROPLANING

##### RUNWAY SURFACE TREATMENTS

Both runway grooving and porous friction course (PFC) antihydroplaning runway surfaces were originated in England, as described in reference 36. Research on runway grooving in the United States started with NASA experiments in 1962 (reported in ref. 2). PFC pavement research in the United States was initiated by USAF (1972) and is reported in references 37 and 38.

## Runway Grooving

Since 1956, approximately 160 runways have been grooved world-wide as indicated in tables 2 to 12. Figure 32 shows the development of grooved runways at U.S. civil airports since the first air carrier airport was grooved in 1967. For the past 3 years an average of 24 air carrier airport runways have been grooved each year. At this present rate, the 224 ILS runways 1524 m (5000 ft) or longer in length at U.S. air carrier airports will all be grooved by 1986. At the present time, six different methods are available for grooving runways, namely, diamond saws, abrasive (carborundum) saws, flails, plastic grooving with segmented drum, plastic grooving with wire comb, and plastic grooving with wire broom. The latter three methods can only be used for grooving portland cement concrete when it has been freshly laid and has not hardened or set up. The most popular grooving method is the diamond saw. Approximately 80 percent of the air carrier airport runways that have been grooved since 1967 have used this grooving method. The effectiveness of runway grooving as an antihydroplaning surface treatment is revealed by reviewing the DBV SDR data shown in tables 13 to 17. Tables 13 to 16 were obtained from reference 39. Table 17 shows data obtained from a recently completed FAA DBV trial application-runway friction calibration and pilot information program (ref. 40). Review of these data suggests that the greatest traction benefit is realized from closed-spaced grooves that are cut 1/4 inch deep in the pavement with diamond saws. This result follows the trend reported in reference 27 where a  $25 \times 6 \times 6$  mm ( $1 \times 1/4 \times 1/4$  in.) pattern was found to be superior to all other patterns studied with regard to preserving traction on wet or flooded runways. Plastic grooving treatments are considered to be an improvement over conventional ungrooved concrete surfaces but are inferior to diamond sawed grooves in both traction performance and water drainage (discussed in section "Flooding on Grooved Runways"). The uniformity of plastic grooving is poor compared with diamond sawed grooves as shown by comparing figures 5 and 6 with figure 33. The data presented in figure 34 compare the traction performance of plastic grooving using a wire comb technique (ref. 41) with other antihydroplaning pavement surface treatments. These data confirm the traction trends just discussed.

The major problem encountered with grooved runways is the chevron cutting of aircraft tires during the touchdown phase of aircraft landings on grooved runways. (See fig. 35.) This problem is discussed in detail in reference 39 and has been studied in reference 42. The civil airlines in the United States at the present time do not consider chevron cutting to be a serious operational problem to their jet transport fleet. It should be noted that the aircraft tire industry has been working in close cooperation with aircraft operators on the chevron cutting problem. During the past 5 years, the aircraft tire industry has developed new tread rubber compounds and tread designs that significantly reduce the degree of chevron cutting on aircraft tires experienced on grooved runways. In this regard, American Airlines reports that over the past 4 years, the number of landings per tire change on its jet transport fleet has increased by 50 percent. During this time period, the number of grooved runways at air carrier airports has increased from 37 to 107. The slipperiness of grooved runways is increased when heavy rubber deposits coat touchdown areas, but this problem is easily corrected by rubber removal treatments (discussed later).

Some asphaltic concrete runways have suffered collapsed grooves in trafficked areas. This type of problem is usually created by grooving the asphaltic concrete shortly after the runway has been paved and before the asphaltic concrete has cured properly.

#### Porous Friction Course

The first PFC surface treatment in the United States was at the Dallas Naval Air Station in 1971 as indicated in table 18. The growth of the PFC surface treatment at U.S. civil airports (through 1975) is shown in figure 36. Over the past 3 years (1973 to 1975), an average of seven air carrier airport runways per year have been given this antihydroplaning pavement surface treatment. Figure 34 shows that this surface is definitely superior in traction qualities over conventional ungrooved concrete and ranks with pavement grooving in this regard as reported in reference 19. PFC has a high storage volume to prevent runway flooding when rain first commences but does not have the free flowing drainage features common to grooved runways. Consequently (as discussed earlier in the paper), PFC surface treatments are not believed to be as effective as grooved pavements, especially those cut with diamond saws, in preventing runway flooding during sustained, high rainfall rate precipitation conditions.

A major problem that has been reported for PFC pavements is the difficulty of removing rubber from contaminated touchdown areas of the runway. AOCI (Airport Operators Council International) reports that the PFC surface at Johannesburg had to be replaced because rubber deposits could not be removed from the surface. A similar problem has been encountered at Denver Stapleton Airport where the rubber deposits could be removed only through the use of a flailing machine and high-pressure water-blast equipment. It should be stressed that the PFC surface treatments at U.S. airports have not been installed long enough at the present time to report realistically on the durability and maintainability of this type pavement surface.

#### Runway Rubber Deposits and Their Removal

NASA, USAF, and FAA studies (tables 13 to 17) show that the most slippery runway segments are usually those located in aircraft touchdown areas which become covered with heavy rubber deposits. The reduced macro/microtexture of the pavement surface (fig. 37) resulting from rubber deposits makes the runway much more susceptible to dynamic and viscous hydroplaning during times of rain. The dramatic runway traction loss suffered as a consequence is illustrated by figure 38. Reference 11 points out that wheel spin-up at touchdown on the Roswell smooth concrete runway (SDR = 2.17 to 2.75 for DRV, B-737, and L-1011) required as much as 2 seconds. From a comparison of figures 13 and 38, the predicted aircraft tire friction coefficient  $\mu_{skid}$  available to spin the tire up on the rubber coated ungrooved runway at MIA runway 9R/27L (SDR = 4.62) is found to be much less than at Roswell. Consequently, wheel spin-up times may take from 6 to 8 seconds on this wet, contaminated surface. As a consequence, pilots may apply wheel braking before the wheels are spun up with the result that the antiskid braking system fails to perform properly and poor braking, poor

directional control along with reverted rubber skidding may occur for the aircraft. (See refs. 8 and 11.) Obviously, runway rubber deposits pose a distinct threat to the operational safety of aircraft during landings and take-offs in adverse weather. This paper has pointed out that ground vehicles which test pavements utilizing a constant speed technique cannot predict the runway slipperiness resulting to aircraft from this effect. Therefore, the DBV, which has a demonstrated capability to perform this measurement, should be the only device permitted to assess this runway condition. Only when test procedures have been changed and the devices correlated or calibrated satisfactorily with the DBV, should other devices be allowed to measure the effects of rubber deposits on runway slipperiness for aircraft operation.

Review of the data contained in tables 13 to 17 and figures 37 and 38 indicates that grooved runways are much less affected by rubber deposits than ungrooved runways and may require less frequent cleaning. Several methods for cleaning runways of rubber deposits are available and discussed in reference 40. One of the most effective means is by high-pressure water blast as shown in figures 39 and 40.

#### CONCLUDING REMARKS

This paper has reviewed the runway slipperiness research performed in the United States and abroad over the time period 1968 to the present. This review suggests that this research has been extremely fruitful with the following tangible benefits resulting to the aviation community:

- (1) A better understanding of the hydroplaning phenomena
- (2) A method for predicting aircraft tire performance on wet runways from a ground-vehicle braking test
- (3) The runway rubber deposit problem has been defined as one of the most serious threats to aircraft operational safety during landings and take-offs in adverse weather; at the same time, methods have been developed which can remove runway rubber deposits so that runway traction is effectively restored to uncontaminated levels
- (4) Pavement grooving has fulfilled its promise as a runway surface treatment that minimizes runway flooding during heavy rainstorms and produces nearly dry aircraft braking and cornering performance under wet runway conditions
- (5) Porous friction course surface treatments are nearly as effective as pavement grooving, but further research and time are required to assess the effects of rubber deposits (and removal), durability, and maintainability of this surface treatment

Finally, it is hoped that this report on the status of runway slipperiness research will stimulate the aviation community and the Federal Regulatory Agencies into a rapid implementation program to utilize the technological advances this research has produced and to improve airport runway safety.

#### REFERENCES

1. Galloway, Bob M.; Schiller, Robert E., Jr.; and Rose, Jerry G.: The Effects of Rainfall Intensity, Pavement Cross Slope, Surface Texture, and Drainage Length on Pavement Water Depths. Res. Rep. No. 138-5, Texas Transp. Inst., Texas A&M Univ., May 1971.
2. Horne, Walter B.; Yager, Thomas J.; and Taylor, Glenn R.: Review of Causes and Alleviation of Low Tire Traction on Wet Runways. NASA TN D-4406, 1968.
3. Horne, Walter B.; and Dreher, Robert C.: Phenomena of Pneumatic Tire Hydroplaning. NASA TN D-2056, 1963.
4. Aircraft Accident Report - Caribbean Atlantic Airlines, Inc.; Douglas DC-9-31, N938PR; Harry S. Truman Airport, Charlotte Amalie, St. Thomas, Virgin Islands; August 12, 1969. Rep. No. NTSB-AAR-70-23, Sept. 16, 1970.
5. Aircraft Accident Report - Piedmont Airlines; Boeing 737, N751N; Greensboro, N.C.; October 28, 1973. Rep. No. NTSB-AAR-74-7, May 22, 1974.
6. Horne, Walter B.; and Joyner, Upshur T.: Determining Causation of Aircraft Skidding Accidents or Incidents. Paper presented at the 23rd Annual International Air Safety Seminar, Flight Safety Foundation, Inc. (Washington, D.C.), Oct. 1970.
7. Horne, Walter B.: Elements Affecting Runway Traction. [Preprint] 740496, Soc. Automat. Eng., Apr.-May 1974.
8. Horne, Walter B.; McCarty, John L.; and Tanner, John A.: Some Effects of Adverse Weather Conditions on Performance of Airplane Antiskid Braking Systems. NASA TN D-8202, 1976.
9. Merritt, Leslie R.: Impact of Runway Traction on Possible Approaches to Certification and Operation of Jet Transport Aircraft. [Preprint] 740497, Soc. Automot. Eng., Apr.-May 1974.
10. Cantu, A. G.; and Chernick, B. E.: Model 737 Data - FAA Evaluation of Proposed Landing Certification Rules. Doc. No. D6-43078, Boeing Co., Dec. 1973.
11. Merritt, Leslie R.: Concorde Landing Requirement Evaluation Tests. Report No. FAA-FS-160-74-2, 1974.
12. Gough, V. E.: Discussion of Paper by D. Tabor, Frottement en Caoutchouc, Rev. Ge'n du Caoutchouc, vol. 36, 1959.
13. Frictional and Retarding Forces on Aircraft Tyres. Part I: Introduction. Eng. Sci. Data Item No. 71025 with amendment A, R. Aeronaut. Soc., Aug. 1972.
14. Leland, Trafford J. W.; Yager, Thomas J.; and Joyner, Upshur T.: Effects of Pavement Texture on Wet-Runway Braking Performance. NASA TN D-4323, 1968.

15. Lander, F. T. W.; and Williams, T.: The Skidding Resistance of Wet Runway Surfaces With Reference to Surface Texture and Tyre Conditions. RRL Rep. LR 184, Road Res. Lab., British Minist. Transp., 1968.
16. Rose, F. G.; Gallaway, R. M.; and Hankins, K. D.: Macrottexture Measurements and Related Skid Resistance at Speeds From 20 to 60 Miles Per Hour. Highway Research Record no. 341, 1970, pp. 33-45.
17. Horne, Walter B.: Skidding Accidents on Runways and Highways Can Be Reduced. Astronaut. & Aeronaut., vol. 5, no. 8, Aug. 1967, pp. 48-55.
18. Expansion of Flight Simulator Capability for Study and Solution of Aircraft Directional Control Problems on Runways. Phase I - Final Report. Rep. MDC A3304 (Contract NAS1-13378), McDonnell Aircraft Co., Mar. 15, 1975. (Available as NASA CR-145084.)
19. Yager, Thomas J.; Phillips, W. Pelham; Horne, Walter B.; and Sparks, Howard C. (appendix D by R. W. Sugg): A Comparison of Aircraft and Ground Vehicle Stopping Performance on Dry, Wet, Flooded, Slush-, Snow-, and Ice-Covered Runways. NASA TN D-6098, 1970.
20. Smiley, Robert F.; and Horne, Walter B.: Mechanical Properties of Pneumatic Tires With Special Reference to Modern Aircraft Tires. NASA TR R-64, 1960. (Supersedes NACA TN 4110.)
21. Horne, Walter B.; and Tanner, John A.: Joint NASA-British Ministry of Technology Skid Correlation Study - Results From American Vehicles. Pavement Grooving and Traction Studies, NASA SP-5073, 1969, pp. 325-359.
22. Sugg, R. W.: Joint NASA-British Ministry of Technology Skid Correlation Study - Results From British Vehicles. Pavement Grooving and Traction Studies, NASA SP-5073, 1969, pp. 361-409.
23. Anon.: Model L-1011-1 (Base Aircraft) Landing Performance Report for FAA Evaluation of Concorde SST Special Condition 25-43-EU-12. Rep. No. LR 26267, Lockheed Aircraft Corp., Jan. 14, 1974.
24. Sugg, R. W.: The Development and Testing of the Runway Friction Meter MK 1 (Mu-Meter). AF/542/043, British Minist. Def., June 1972.
25. Merritt, L. R.: Analysis of Tests Conducted by the French Ministry of Armed Forces Flight Test Center for the Service Technique Aeronautique (STAE) Utilizing a Caravelle 116 Aircraft and a Diagonal Braked Vehicle (DBV). Rep. No. FS-160-75-2, FAA, Oct. 1975.
26. Blanchard, J. W.: An Analysis of the B727 and DC9 Trials on Wet Runways With the Mu-Meter and Diagonal Braked Vehicle (DBV). Civil Aviat. Auth. (London), Dec. 1974.

27. Yager, Thomas J.: Comparative Braking Performance of Various Aircraft on Grooved and Ungrooved Pavements at the Landing Research Runway, NASA Wallops Station. Pavement Grooving and Traction Studies, NASA SP-5073, 1969, pp. 35-65.
28. Williams, John H.: Analysis of the Standard USAF Runway Skid Resistance Tests. AFCEC-TR-75-3, U.S. Air Force, May 1975.
29. Nussbaum, Peter J.; Hierung, William A.; and Grisel, Charles R.: Runway Friction Data for 10 Civil Airports as Measured With a Mu-Meter and Diagonal Braked Vehicle. Rep. No. FAA-RD-72-61, July 1972.
30. Horne, Walter B.: Results From Studies of Highway Grooving and Texturing at NASA Wallops Station. Pavement Grooving and Traction Studies, NASA SP-5073, 1969, pp. 425-464.
31. Van Eldik Thieme, H. C. A.: Cornering and Camber Experiments. Mechanics of Pneumatic Tires, Samuel K. Clark, ed., NBS Monogr. 122, U.S. Dep. Commer., Nov. 1971, pp. 631-693.
32. Preston, O. W.; Kibbee, G. W.; Muroyama, R. H.; and Storley, R. A.: Development of a Basic Methodology for Predicting Aircraft Stopping Distance on a Wet Runway. Rep. No. FAA-RD-70-62, Mar. 1971.
33. Ballentine, George D.; and Compton, Phil V.: Procedures for Conducting the Air Force Weapons Laboratory Standard Skid Resistance Test. AFWL-TR-73-165, U.S. Air Force, Sept. 1973.
34. AFCEC Pavement Surface Effects Team: Runway Skid Resistance Survey Report. Air Force Civil Eng. Center, U.S. Air Force, 1975.  
Production FLT/Test Instln, AF Plant 42, Palmdale, California, Mar. 1975.  
Norton AFB, California, Apr. 1975.  
March AFB, California, Apr. 1975.  
Vandenberg AFB, California, Apr. 1975.  
Williams AFB, California, Apr. 1975.  
Davis Monthan AFB, Arizona, Apr. 1975.  
Reese AFB, Texas, May 1975.  
Carswell AFB, Texas, May 1975.  
Dress AFB, Texas, May 1975.  
Webb AFB, Texas, May 1975.  
Laughlin AFB, Texas, May 1975.  
Randolph AFB, Texas, May 1975.  
Barksdale AFB, Louisiana, May 1975.  
Yokota AFB, Japan, Aug. 1975.  
Elmendorf AFB, Alaska, Aug. 1975.
35. Methods for the Design, Construction, and Maintenance of Skid Resistant Airport Pavement Surfaces. AC No. 150/5320-12, FAA, June 30, 1975.
36. Martin, F. R.: Pavement Surface Treatments at Airports in Great Britain. Pavement Grooving and Traction Studies, NASA SP-5073, 1969, pp. 235-278.

37. Tomita, Hisao; and Forrest, J. B.: Porous Friction Surfaces for Airfield Pavements. AFWL-TR-74-177, U.S. Air Force, May 1975.
38. Compton, Phil V.; and Hargett, Emil R.: Skid-Resistance Evaluation of Seven Antihydroplaning Surfaces. AFWL-TR-74-54, U.S. Air Force, May 1974.
39. Horne, Walter B.; and Griswold, Guy D.: Evaluation of High Pressure Water Blast With Rotating Spray Bar for Removing Paint and Rubber Deposits From Airport Runways, and Review of Runway Slipperiness Problems Created by Rubber Contamination. NASA TM X-72797, 1975.
40. Merritt, Leslie R.: Trial Application-Runway Friction Calibration and Pilot Information Program. Rep. No. AFS-160-76-1, FAA, Aug. 19, 1976.
41. Marlin, Eugene C.; and Horne, Walter B.: Plastic (Wire-Combed) Grooving of a Slip-Formed Concrete Runway Overlay at Patrick Henry Airport - An Initial Evaluation. Paper presented at the Southeastern Airport Managers Association (Fort Lauderdale, Fla.), Nov. 1973.
42. Byrdsong, Thomas A.; McCarty, John Locke; and Yager, Thomas J.: Investigation of Aircraft Tire Damage Resulting From Touchdown on Grooved Runway Surfaces. NASA TN D-6690, 1972.

KEY TO ABBREVIATIONS USED IN TABLES

Abbreviation	Meaning
AB	Air Base
AC	Asphaltic concrete
AFB	Air Force Base
AFCEC	Air Force Civil Engineering Center
ASTM	American Society for Testing and Materials
ATD	Average texture depth
C	Civil
CS	Carborundum saw
D	Depth
DBV	Diagonal-braked vehicle
DS	Diamond saw
F	Flail
FAA	Federal Aviation Administration
G	Grooved
Int.	International
L	Longitudinal
Lt	Light
M	Military
Med	Medium
Metro.	Metropolitan
Mun.	Municipal
N/A	Not available
NAS	Naval Air Station
Nat.	National
P	Pitch
PCC	Portland cement concrete
PGSD	Plastic grooving with segmented drum
PGWB	Plastic grooving with wire broom
PGWC	Plastic grooving with wire comb
RAF	Royal Air Force
SDR	Stopping distance ratio
T	Transverse
W	Width

TABLE 1.- TIRE CHARACTERISTICS OF FRICTION MEASURING DEVICES

Device	$\mu_{dry}$	P	
		kPa	lb/in <sup>2</sup>
DBV (ASTM E-249 smooth tread tire) . . . . .	1.15	165	24
DBV (ASTM E-524 smooth tread tire) . . . . .	1.20	165	24
Mu-Meter . . . . .	0.84	69	10
Miles trailer . . . . .	1.15	138	20
Skiddometer model BV-6 (ASTM E-249 smooth tread tire). . .	1.15	165	24

TABLE 2.- GROOVED RUNWAYS CONSTRUCTED DURING 1956-1966

Airport	Country	Runway	Surface	Grooving technique	Groove pattern, P x W x D	
					mm	in.
A (1956) - M	UK	N/A	AC	T-F	25 x 3 x 3	1 x 1/8 x 1/8
B (1957) - M	UK	N/A	AC	T-F	25 x 3 x 3	1 x 1/8 x 1/8
C (1960) - M	UK	N/A	AC	T-F	25 x 3 x 3	1 x 1/8 x 1/8
D (1960) - M	UK	N/A	AC	T-F	25 x 3 x 3	1 x 1/8 x 1/8
E (1960) - M	UK	N/A	PCC	T-F	25 x 3 x 3	1 x 1/8 x 1/8
F (1961) - M	UK	N/A	AC	T-CS	25 x 3 x 3	1 x 1/8 x 1/8
Manchester (1961) - C	UK	N/A	AC	T-F	25 x 3 x 3	1 x 1/8 x 1/8
NASA LaRC (1964) - C	USA	Research track	AC	T-DS	25 x 3 x 3	1 x 1/8 x 1/8
			PCC	L-DS	25 x 6 x 6	1 x 1/4 x 1/4
Manchester (1965) - C	UK	N/A	AC	T-F	25 x 3 x 3	1 x 1/8 x 1/8
Ubon (1966) - M	USA	N/A	PCC	T-DS	51 x 6 x 6 (Skip 610)	2 x 1/4 x 1/4 (Skip 24)
Udorn (1966) - M	USA	N/A	PCC	T-DS	51 x 6 x 6 (Skip 610)	2 x 1/4 x 1/4 (Skip 24)
					25 x 3-9 x 3	1 x 1/8-3/8 x 1/8
NASA LaRC (1966) - C	USA	Research track	PCC	T-F	38 x 3-9 x 3	1 1/2 x 1/8-3/8 x 1/8
					51 x 3-9 x 3	2 x 1/8-3/8 x 1/8
				T-DS	75 x 3-9 x 6	1 x 1/8-3/8 x 1/4
					38 x 3-9 x 6	1 1/2 x 1/8-3/8 x 1/4
51 x 3-9 x 6	2 x 1/3-3/8 x 1/4					

TABLE 3.- GROOVED RUNWAYS CONSTRUCTED DURING 1967

Airport	Country	Runway	Surface	Grooving technique	Groove pattern, P x W x D	
					mm	in.
Bien Hoa - M	USA	N/A	PCC	T-DS	51 x 6 x 6 (Skip 610)	2 x 1/4 x 1/4 (Skip 24)
Birmingham - C	UK	N/A	AC	T-F	25 x 3 x 3	1 x 1/8 x 1/8
Beale AFB - M	USA	14/32	PCC	T-DS	25 x 6 x 6	1 x 1/4 x 1/4
John F. Kennedy - C	USA	4R/22L	PCC	T-DS	38 x 10-5 x 3	1 1/2 x 3/8-3/16 x 1/8
Kansas City Mun. - C	USA	18/36	PCC/AC	T-DS	25 x 3 x 6	1 x 1/8 x 1/4
NASA Wallops - C	USA	4/22	PCC/AC	T-DS	25 x 6 x 6	1 x 1/4 x 1/4
Washington Nat. - C	USA	18/36	AC	T-DS	25 x 3 x 3	1 x 1/8 x 1/8

TABLE 4.- GROOVED RUNWAYS CONSTRUCTED DURING 1968

Airport	Country	Runway	Surface	Grooving technique	Groove pattern, P x W x D	
					mm	in.
Atlanta Mun. - C	USA	9R/27L	PCC	T-DS	32 x 10-3 x 6	1 1/4 x 3/8-1/8 x 1/4
Chicago-Midway - C	USA	13R/31L	PCC	T-DS	32 x 6 x 6	1 1/4 x 1/4 x 1/4
Chicago-Midway - C	USA	4R/22L	PCC	T-DS	32 x 6 x 6	1 1/4 x 1/4 x 1/4
Seymour-Johnson AFB - M	USA	8/26	PCC/AC	T-DS	51 x 6 x 6 (Skip 610)	2 x 1/4 x 1/4 (Skip 24)
Tempelhof (Ger.) - M	USA	9R/27L	AC	T-DS	38 x 10 x 10	1 1/2 x 3/8 x 3/8

ORIGINAL PAGE IS  
OF POOR QUALITY

TABLE 5.- GROOVED RUNWAYS CONSTRUCTED DURING 1969

Airport	Country	Runway	Surface	Grooving technique	Groove pattern, P x W x D	
					mm	in.
Boston Logan - C	USA	N/A	AC	T-DS	25 x 6 x 6	1 x 1/4 x 1/4
Charleston (W.Va.) - C	USA	5/23	PCC/AC	T-DS	32 x 6 x 6	1 1/4 x 1/4 x 1/4
Chicago O'Hare - C	USA	9L/27R	PCC/AC	T-DS	32 x 6 x 6	1 1/4 x 1/4 x 1/4
Dallas Love Field - C	USA	13R/31L	PCC	T-DS	32 x 6 x 6	1 1/4 x 1/4 x 1/4
Offutt AFB - M	USA	12/30	PCC	T-DS	32 x 6 x 6	1 1/4 x 1/4 x 1/4
Wellington - C	New Zealand	N/A	AC	T-DS	25 x 3 x 3	1 x 1/8 x 1/8

TABLE 6.- GROOVED RUNWAYS CONSTRUCTED DURING 1970

Airport	Country	Runway	Surface	Grooving technique	Groove pattern, P x W x D	
					mm	in.
Bangkok	Thailand	N/A	PCC	T-DS	51 x 6 x 6	2 x 1/4 x 1/4
Dallas Love Field - C	USA	13L/31R	AC	T-DS	38 x 10 x 6	1 1/2 x 3/8 x 1/4
Harry S. Truman - C	USA	9/27	PCC/AC	T-DS/CS	38 x 10 x 6	1 1/2 x 1/4 x 1/4
Kadena - M	USA	N/A	PCC/AC	T-DS	32 x 6 x 6	1 1/4 x 1/4 x 1/4
Nashville Met. - C	USA	2L/20R	AC	T-DS/CS	51 x 6 x 6	2 x 1/4 x 1/4
Nashville Met. - C	USA	13/31	PCC/AC	T-DS/CS	32 x 6 x 6	1 1/4 x 1/4 x 1/4
Orly - C	France	N/A	PCC	T-DS	N/A	N/A
Port Hardy - C	Canada	N/A	AC	T-DS	25 x 6 x 6	1 x 1/4 x 1/4
Shemya - M	USA	10/28	AC	T-DS	32 x 6 x 6	1 1/4 x 1/4 x 1/4

TABLE 7.- GROOVED RUNWAYS CONSTRUCTED DURING 1971

Airport	Country	Runway	Surface	Grooving technique	Groove pattern, P x W x D	
					mm	in.
Boston Logan - C	USA	4R/22L	AC	T-DS	57 x 6 x 6	2 1/4 x 1/4 x 1/4
Chicago O'Hare - C	USA	4R/22L	PCC	T-DS	32 x 6 x 6	1 1/4 x 1/4 x 1/4
Houston Int. - C	USA	8L/26R	PCC	T-DS	51 x 6 x 6	2 x 1/4 x 1/4
Kaitak - C	Hong Kong	13/31	PCC/AC	T-DS	44 x 6 x 6	1 3/4 x 1/4 x 1/4
Kansan - M	USA	17/35	PCC	T-DS	32 x 6 x 6	1 1/4 x 1/4 x 1/4
LaGuardia - C	USA	4/22	AC	T-DS	38 x 10-5 x 5	1 1/2 x 3/8-3/16 x 3/16
LaGuardia - C	USA	13/31	AC	T-DS	38 x 10-5 x 5	1 1/2 x 3/8-3/16 x 3/16
Memphis Int. - C	USA	17R/35L	PCC	T-PCWB	N/A	N/A
Newark - C	USA	4L/22R	AC	T-DS	38 x 10-5 x 5	1 1/2 x 3/8-3/16 x 3/16
San Diego Lindberg - C	USA	9/27	PCC	T-DS	25 x 6 x 6	1 x 1/4 x 1/4
Springfield (Ill.) - C	USA	4/22	PCC	T-DS	32 x 6 x 6	1 1/4 x 1/4 x 1/4
Tampa Int. - C	USA	18L/30R	PCC	T-PCWB	N/A	N/A

TABLE 8.- GROOVED RUNWAYS CONSTRUCTED DURING 1972

Airport	Country	Runway	Surface	Grooving technique	Groove pattern, P x W x D	
					mm	in.
Baton Rouge - C	USA	4/22	PCC	T-PG	51 x 6 x 6	2 x 1/4 x 1/4
Boston Logan - C	USA	4R/22L	AC	T-DS	57 x 8 x 6	2 1/4 x 5/16 x 1/4
Cincinnati - C	USA	18/36	AC	T-DS	38 x 6 x 6	1 1/2 x 1/4 x 1/4
Cincinnati - C	USA	9R/27L	PCC	T-DS	38 x 6 x 6	1 1/2 x 1/4 x 1/4
Denver Stapleton - C	USA	17L/35R	PCC	T-DS	51 x 6 x 6	2 x 1/4 x 1/4
Detroit Met. - C	USA	3L/21R	PCC	T-DS	32 x 6 x 6	1 1/4 x 1/4 x 1/4
Minneapolis - C	USA	4/22	PCC	T-DS	51 x 6 x 6	2 x 1/4 x 1/4
Oklahoma City - C	USA	17R/35L	PCC	T-PG	25 x 13 x 13	1 x 1/2 x 1/2
Omaha Eppley Field - C	USA	14R/32L	AC	T-DS	32 x 6 x 6	1 1/4 x 1/4 x 1/4
Osan - M	USA	9/27	PCC	T-DS	32 x 6 x 6	1 1/4 x 1/4 x 1/4
Plattsburg - M	USA	17/35	PCC	T-DS	38 x 6 x 6	1 1/2 x 1/4 x 1/4
Shaw - M	USA	4L/22R	PCC	T-DS	51 x 6 x 6	2 x 1/4 x 1/4
Springfield (Mo.) - C	USA	1/19	PCC	T-DS	(Skip 610)	(Skip 24)
St. Paul Holman - C	USA	12/30	AC	T-DS	51 x 6 x 6	2 x 1/4 x 1/4
Waterloo Mun. - C	USA	12/30	PCC	T-DS	32 x 6 x 6	1 1/4 x 1/4 x 1/4
Washington Nat. - C	USA	18/36	AC	T-DS	32 x 6 x 6	1 1/4 x 1/4 x 1/4

TABLE 9.- GROOVED RUNWAYS CONSTRUCTED DURING 1973

Airport	Country	Runway	Surface	Grooving technique	Groove pattern, P x W x D	
					mm	in.
Allentown - C	USA	6/24	AC	T-DS	32 x 6 x 6	1 1/4 x 1/4 x 1/4
Atlanta Int. - C	USA	9R/27L	PCC	T-PGWC	N/A	N/A
Baltimore Int. - C	USA	10/28	AC	T-DS	32 x 6 x 6	1 1/4 x 1/4 x 1/4
Baltimore Int. - C	USA	15/33	AC	T-DS	32 x 6 x 6	1 1/4 x 1/4 x 1/4
Charles DeGaulle - C	France	N/A	PCC	T-DS	N/A	N/A
Clarksburg - C	USA	3/21	AC	T-DS	51 x 6 x 6	2 x 1/4 x 1/4
Cleveland Hopkins - C	USA	5R/23L	AC	T-DS	38 x 6 x 6	1 1/2 x 1/4 x 1/4
Dallas/Ft. Worth - C	USA	17L/35R	PCC	T-DS	38 x 6 x 6	1 1/2 x 1/4 x 1/4
Dallas/Ft. Worth - C	USA	17R/35L	PCC	T-DS	38 x 6 x 6	1 1/2 x 1/4 x 1/4
Dallas/Ft. Worth - C	USA	13L/31R	PCC	T-DS	38 x 6 x 6	1 1/2 x 1/4 x 1/4
Gainesville Mun. - C	USA	10/28	AC	T-DS	38 x 6 x 6	1 1/2 x 1/4 x 1/4
Griffiss - M	USA	15/33	PCC	T-DS	51 x 6 x 6	2 x 1/4 x 1/4
Huntington - C	USA	12/30	AC	T-DS	32 x 6 x 6	1 1/4 x 1/4 x 1/4
Jacksonville Int. - C	USA	7/25	AC	T-DS	51 x 6 x 6	2 x 1/4 x 1/4
Lafayette (Ind.) - C	USA	10/28	AC	T-DS	32 x 6 x 6	1 1/4 x 1/4 x 1/4
LaGuardia - C	USA	13/31	AC	T-DS	38 x 10-5 x 5	1 1/2 x 3/8-3/16 x 3/16
Miami Int. - C	USA	9L/27R	AC	T-DS	38 x 6 x 6	1 1/2 x 1/4 x 1/4
Miami Int. - C	USA	9R/27L	AC	T-DS	38 x 6 x 6	1 1/2 x 1/4 x 1/4
Patrick Henry Field - C	USA	6/24	PCC	T-PGWC	13 x 3 x 3	1/2 x 1/8 x 1/8
Peoria (Ill.) - C	USA	12/30	AC	T-DS	51-76 x 6 x 6	2-3 x 1/4 x 1/4
Savannah - C	USA	18/36	PCC	T-PGWC	N/A	N/A
Scuth Bend - C	USA	9/27	AC	T-DS	32 x 6 x 6	1 1/4 x 1/4 x 1/4
St. Louis Lambert - C	USA	6/24	PCC	T-DS	32 x 6 x 6	1 1/4 x 1/4 x 1/4
Vance - M	USA	17R/35L	PCC	T-DS	51 x 6 x 6	2 x 1/4 x 1/4
Williamsport - C	USA	9/27	AC	T-DS	32 x 6 x 6	1 1/4 x 1/4 x 1/4

ORIGINAL PAGE IS  
OF POOR QUALITY

TABLE 10.- GROOVED RUNWAYS CONSTRUCTED DURING 1974

Airport	Country	Runway	Surface	Grooving technique	Groove pattern, P x W x D	
					mm	in.
Aibany (N.Y.) - C	USA	10/28	AC	T-DS	32 x 6 x 6	1 1/4 x 1/4 x 1/4
Allentown - C	USA	13/31	AC	T-DS	38 x 6 x 6	1 1/2 x 1/4 x 1/4
Bagotville - M	Canada	11/29	PCC	T-PGWC	N/A	N/A
Bangor - C	USA	15/33	PCC	T-DS	32 x 6 x 6	1 1/4 x 1/4 x 1/4
Cedar Rapids - C	USA	8/26	AC	T-DS	32 x 6 x 6	1 1/4 x 1/4 x 1/4
Cedar Rapids - C	USA	13/31	AC	T-DS	32 x 6 x 6	1 1/4 x 1/4 x 1/4
Chattanooga - C	USA	2R/20L	AC	T-DS	38 x 6 x 6	1 1/2 x 1/4 x 1/4
Chicago O'Hare - C	USA	14L/32R	AC	T-DS	32 x 6 x 6	1 1/4 x 1/4 x 1/4
Chicago O'Hare - C	USA	14R/32L	AC	T-DS	32 x 6 x 6	1 1/4 x 1/4 x 1/4
Chicago O'Hare - C	USA	9R/27L	AC	T-DS	32 x 6 x 6	1 1/4 x 1/4 x 1/4
Cleveland Hopkins - C	USA	10L/28R	AC	T-DS	38 x 6 x 6	1 1/2 x 1/4 x 1/4
England - M	USA	14/32	PCC	T-DS	51 x 6 x 6 (Skip 610)	2 x 1/4 x 1/4 (Skip 24)
Elsworth - M	USA	12/30	AC	T-DS	38 x 6 x 6	1 1/2 x 1/4 x 1/4
Harry S. Truman - C	USA	9/27	AC	T-DS	51 x 10 x 6	2 x 3/8 x 1/4
Jacksonville Int. - C	USA	7/25	AC	T-DS	51 x 6 x 6	2 x 1/4 x 1/4
John F. Kennedy - C	USA	13L/31R	AC	T-DS	38 x 10-5 x 5	1 1/2 x 3/8-3/16 x 3/16
John F. Kennedy - C	USA	4L/22R	PCC/AC	T-DS	38 x 10-5 x 5	1 1/2 x 3/8-3/16 x 3/16
Lawton - C	USA	17/35	PCC	T-PG	51 x 6 x 3	2 x 1/4 x 1/8
Los Angeles Int. - C	USA	6R/24L	PCC/AC	T-DS	38 x 6 x 6	1 1/2 x 1/4 x 1/4
Louisville - C	USA	1/19	PCC	T-PGWB	N/A	N/A
Memphis Int. - C	USA	17L/35R	PCC	T-PGWB	N/A	N/A
Minneapolis - C	USA	11R/29L	PCC/AC	T-DS	32 x 6 x 6	1 1/4 x 1/4 x 1/4
Newark - C	USA	4R/22L	AC	T-DS	36 x 10-5 x 5	1 1/2 x 3/8-3/16 x 3/16
Patrick Henry Field - C	USA	2/20	PCC	T-PGWC	13 x 3 x 3	1/2 x 1/8 x 1/8
Pittsburg - C	USA	10L/28R	PCC	T-DS	32 x 5 x 6	1 1/4 x 1/4 x 1/4
Ponca City - C	USA	17/35	PCC	T-PG	51 x 6 x 3	2 x 1/4 x 1/8
Washington Nat. - C	USA	18/36	AC	T-DS	32 x 6 x 6	1 1/4 x 1/4 x 1/4

TABLE 11.- GROOVED RUNWAYS CONSTRUCTED DURING 1975

Airport	Country	Runway	Surface	Grooving technique	Groove pattern, P x W x D	
					mm	in.
Arlanda - C	Sweden	N/A	PCC*	N/A	25 x 3 x 3	1 x 1/8 x 1/8
Beaumont - C	USA	11/29	PCL	T-PC	51 x 6 x 6	2 x 1/4 x 1/4
Boston Logan - C	USA	4L/22R	AC	T-DS	57 x 6 x 6	2 1/4 x 1/4 x 1/4
Boston Logan - C	USA	15R/33L	AC	T-DS	57 x 6 x 6	2 1/4 x 1/4 x 1/4
Cannon - M	USA	3/21	PCC	T-DS	57 x 6 x 6 (Skip 610)	2 x 1/4 x 1/4 (Skip 24)
Charlotte - C	USA	5/23	PCC/AC	T-DS	44 x 6 x 6	1 3/4 x 1/4 x 1/4
Chicago O'Hare - C	USA	9L/27R	AC	T-DS	32 x 6 x 6	1 1/4 x 1/4 x 1/4
Chicago O'Hare - C	USA	4L/22R	AC	T-DS	32 x 6 x 6	1 1/4 x 1/4 x 1/4
Denver Stapleton - C	USA	17L/35R	PCC	T-DS	51 x 6 x 6	2 x 1/4 x 1/4
Des Moines Mun. - C	USA	12L/30R	AC	T-DS	32 x 6 x 6	1 1/4 x 1/4 x 1/4
Dunedin - C	New Zealand	N/A	N/A	N/A	N/A	N/A
Elmira - C	USA	10/28	AC	T-DS	32 x 6 x 6	1 1/4 x 1/4 x 1/4
Eria - C	USA	6/24	AC	T-DS	51 x 6 x 6	2 x 1/4 x 1/4
Fort Lauderdale - C	USA	9L/27R	AC	T-DS	38 x 6 x 6	1 1/2 x 1/4 x 1/4
Grand Forks - M	USA	17/35	PCC	T-DS	51 x 6 x 6	2 x 1/4 x 1/4
Houston Int. - C	USA	14/32	PCC	T-PC	51 x 6 x 6	2 x 1/4 x 1/4
Invercargill - C	New Zealand	N/A	N/A	N/A	N/A	N/A
Kansas City Int. - C	USA	9/27	PCC	T-DS	32 x 6 x 6	1 1/4 x 1/4 x 1/4
Kansas City Int. - C	USA	1/19	PCC/AC	T-DS	32 x 6 x 6	1 1/4 x 1/4 x 1/4
Kincheloe - M	USA	15/33	PCC	T-DS	51 x 6 x 6	2 x 1/4 x 1/4
Knoxville - C	USA	4L/22R	PCC	T-PGWB	N/A	N/A
Lubbock Int. - C	USA	8/26	PCC	T-DS	32 x 6 x 6	1 1/4 x 1/4 x 1/4
Monroe (La.) - C	USA	4/22	PCC	T-PC	13 x 6 x 3	1/2 x 1/4 x 1/8
New Haven - C	USA	2/20	AC	T-DS	48 x 6 x 6	1 7/8 x 1/4 x 1/4
Pittsburg - C	USA	14/32	PCC/AC	T-DS	32 x 6 x 6	1 1/4 x 1/4 x 1/4
Pittsburg - C	USA	10R/28L	PCC	T-DS	32 x 6 x 6	1 1/4 x 1/4 x 1/4
San Antonio - C	USA	12R/30L	PCC	T-PC	51 x 6 x 6	2 x 1/4 x 1/4
Tallahassee - C	USA	13/36	AC	T-DS	44 x 6 x 6	1 3/4 x 1/4 x 1/4
Tampa - C	USA	18R/36L	AC	T-DS	4 x 6 x 6	1 3/4 x 1/4 x 1/4
Washington Nat. - C	USA	15/33	AC	T-DS	32 x 6 x 6	1 1/4 x 1/4 x 1/4
Wilkes-Barre - C	USA	4/22	AC	T-DS	38 x 6 x 6	1 1/2 x 1/4 x 1/4
Victoria Int. - C	Canada	N/A	N/A	N/A	N/A	N/A
Zurich - C	Switzerland	N/A	N/A	N/A	N/A	N/A

TABLE 12.- GROOVED RUNWAYS CONSTRUCTED DURING 1976

Airport	Country	Runway	Surface	Grooving technique	Groove pattern, P x W x D	
					mm	in.
Albany County - C	USA	N/A	AC	T-DS	32 x 5 x 6	1 1/4 x 1/4 x 1/4
Boston Logan - C	USA	N/A	AC	T-DS	57 x 6 x 6	2 1/4 x 1/4 x 1/4
Cumberland (Md.) - C	USA	N/A	N/A	T-DS	N/A	N/A
Jackson County (W.Va.) - C	USA	N/A	AC	T-DS	32 x 6 x 6	1 1/4 x 1/4 x 1/4
Ithue (H.I.) - C	USA	N/A	AC	T-DS	44 x 6 x 6	1 3/4 x 1/4 x 1/4
NASA Kennedy - C	USA	N/A	PCC	T-DS	29 x 6 x 6	1 1/8 x 1/4 x 1/4
Raleigh Heights (W.Va.) - C	USA	N/A	PCC/AC	T-DS	32 x 6 x 6	1 1/4 x 1/4 x 1/4
Wood County (W.Va.) - C	USA	N/A	AC	T-DS	38 x 6 x 6	1 1/2 x 1/4

ORIGINAL PAGE IS  
OF POOR QUALITY

TABLE 13.- DBV SDR AND NASA GREASE TEST ATD OBTAINED ON RUNWAYS

EVALUATED JULY 1973 TO DECEMBER 1974 BY AFCEC  
 [From reference 28]

Airfield	Runway	Surface	Touchdown area, rubber deposits			Trafficked, no rubber			Untrafficked, no rubber		
			SDR (a)	ATD		SDR (a)	ATD		SDR (a)	ATD	
				mm	in.		mm	in.		mm	in.
Travis	21L	PCC	5.79	0.37 <sup>a</sup>	0.0148	2.28	0.9677	0.0381	---	---	---
Fairchild	23	PCC	4.75	.1092	.0043	1.97	.4318	.0170	1.97	0.2769	0.0109
Castle	30	AC	4.60	.1448	.0357	2.00	---	---	1.59	.8306	.0327
Loring	01	AC	4.58	.1499	.0059	1.99	.3632	.0143	---	---	---
Travis	21R	AC	4.01	.3632	.0143	2.71	.4140	.0163	2.18	.5537	.0218
McGuire	24	AC	3.92	.1575	.0062	1.93	.3073	.0121	1.33	---	---
Torrejon	23	AC	3.85	.1626	.0064	1.85	.5333	.0450	1.50	.6452	.0254
Mather	22L	PCC/AC	3.75	.2083	.0082	1.86	---	.0163	---	---	---
Blytheville	17	PCC	3.73	---	---	---	---	---	1.57	---	---
Dover	01	PCC/AC	3.62	---	---	1.74	---	---	1.47	---	---
Scott	31	AC	3.61	---	---	1.83	---	---	1.47	---	---
Robbins	32	PCC	3.59	.2896	.0114	2.01	.4928	.0194	---	---	---
Cannon	21	PCC/GPCC	3.59	---	---	1.74	---	---	1.43	---	---
Rickenbacker	23L	PCC	3.40	.2769	.0109	2.04	.4851	.0190	1.86	.5055	.0199
Homestead	05	PCC	3.37	.2235	.0088	1.92	.7061	.0278	2.17	.4140	.0163
Grisson	22	AC	3.23	.1041	.0041	1.66	.5055	.0199	1.60	.5283	.0208
Charleston	15	AC/PCC	3.21	.2159	.0085	2.55	---	---	2.21	.3302	.0130
Zaragoza	31R	AC	2.93	.2591	.0102	1.31	.5817	.0229	1.32	.5537	.0218
Mather	22R	AC	2.90	.2083	.0082	2.18	.4140	.0163	1.67	---	---
Andrews	01L	PCC	2.89	.4064	.0160	2.14	.5588	.0220	2.28	.9398	.0370
Charleston	21	AC	2.79	.3327	.0131	1.88	.5817	.0229	---	---	---
Shaw	4L	PCC/GPCC/AC	2.77	.3429	.0135	1.79	.7264	.0286	1.52	.4851	.0191
McConnel	18R	AC	2.77	---	---	2.03	---	---	---	---	---
Hector	35	PCC	2.72	---	---	1.95	.6121	.0241	1.89	---	---
Dover	31	AC	2.66	---	---	1.89	---	---	1.28	---	---
Columbus	13L	PCC/AC	2.62	.4851	.0191	1.80	.4851	.0191	1.71	.5537	.0218
Clasgow	28	PCC	2.61	.3632	.0143	2.11	.2464	.0097	2.37	.1727	.0068
Andrews	01R	PCC/AC	2.60	.3302	.0130	1.73	.635	.025	1.8.	.686	.027
England	14	PCC	2.54	---	---	2.66	.5055	.0199	---	---	---
Aviano	05	AC	2.51	.889	.035	1.73	1.168	.046	1.84	.965	.038
R. Gebaur	36	PCC/AC	2.50	---	---	2.22	---	---	2.29	---	---
Vance	17R	PCC/AC/GPCC	2.50	---	---	1.50	---	---	1.53	---	---
Soesterberg	28	AC	2.42	---	---	2.29	---	---	1.57	---	---
Columbus	13R	PCC	2.40	---	---	2.28	---	---	---	---	---
England	18	PCC/AC	2.39	.6452	.0254	2.57	.6375	.0251	2.40	---	---
Moody	18R	PCC/AC	2.38	.4851	.0191	1.48	1.1633	.0458	1.32	1.1633	.0458
Zweibrucken	03	AC	2.34	.5283	.0208	1.35	.8941	.0352	1.16	.7264	.0286
Bentwaters	25	PCC/AC	2.33	.4851	.0191	1.44	1.1633	.0458	1.57	.6121	.0241
Moody	18L	PCC/AC	2.32	.3073	.0121	1.66	.5283	.0208	1.45	.6121	.0241
Craig	32L	PCC/AC	2.27	.4318	.0170	1.70	.3327	.0131	1.42	1.3462	.0530
Rickenbacker	23R	AC	2.26	---	---	1.94	---	---	---	---	---
Vance	17C	PCC/AC	2.25	.1448	.0057	1.45	.8941	.0352	1.52	---	---
Columbus	13C	PCC/AC	2.22	---	---	1.90	---	---	2.13	---	---
Woodbridge	27	AC	2.22	---	---	1.53	---	---	2.01	---	---
Niagara Falls	28	AC	2.12	.1651	.0065	1.80	.4351	.0191	1.28	.6121	.0241
Vance	17L	PCC	2.10	---	---	2.09	.4851	.0191	---	---	---
McConnel	18L	AC	2.03	---	---	1.73	---	---	1.89	---	---
McGuire	36	PCC/AC	2.00	.1575	.0062	1.66	.3023	.0121	1.36	---	---
Myrtle Beach	17	PCC/AC	2.00	.4013	.0158	1.57	.5283	.0208	1.52	.6452	.0254
Cannon	30	PCC/AC	2.00	---	---	1.65	---	---	1.81	---	---
Shaw	04R	PCC/GPCC/PCC	1.99	.3150	.0124	1.13	1.5570	.0613	1.38	---	---
Erding	26	PCC	1.93	.2184	.0086	2.04	.4851	.0191	1.73	.4470	.0176
Hurlburt	35	PCC/AC	1.89	.5055	.0199	1.92	.6832	.0269	1.34	.8306	.0327
McChord	34	AC	1.87	.7747	.0305	2.23	.8306	.0327	2.13	.7747	.0305

<sup>a</sup> DBV SDR: 3 minutes after wetting.

TABLE 14.- DBV SDR OBTAINED ON RUNWAYS EVALUATED JANUARY TO JUNE 1975 BY AFCEC  
 [From reference 38]

Airfield	Runway	Rubber-coated touchdown areas				Trafficked, no rubber (wheel paths)		Untrafficked, no rubber (runway edge)	
		Primary		Secondary		SDR (a)	Surface	SDR (a)	Surface
		SDR (a)	Surface	SDR (a)	Surface				
Palmdale	07/25	6.12	PCC	2.55	PCC	2.31	PCC	----	PCC/AC
March	13/31	5.19	PCC	2.46	PCC	2.21	FCC	----	AC
Barksdale	14/32	4.73	AC	3.70	AC	1.84	AC	1.40	AC
Norton	05/23	4.58	PCC	2.75	PCC	2.19	PCC	2.40	PCC
<sup>b</sup> Webb	17L/35R	2.95	PCC/AC	1.51	PCC/AC	4.51	AC	----	AC
Dyess	16/34	3.52	PCC	4.46	PCC	2.61	PCC	----	AC
Carswell	17/35	2.78	AC/PCC	4.11	FCC	2.36	AC/PCC	1.32	AC
Elmendorf	05/23	3.53	AC	1.92	AC	2.95	AC	1.52	AC
Reese	17R/35L	3.03	PCC	1.85	PCC/AC	1.80	PCC/AC	1.72	AC
Davis Monthan	12/30	2.98	AC	2.50	FCC	1.54	AC	1.39	AC
Palmdale	04/22	2.88	AC	2.43	AC	1.82	AC	2.05	AC
<sup>b</sup> Webb	17R/35L	2.82	PCC/AC	2.65	PCC/AC	2.69	AC	----	AC
Laughlin	13C/31C	2.70	PCC/AC	1.88	PCC/AC	1.69	AC	1.75	AC
Randolph	14L/32R	2.65	PCC	2.16	PCC	2.05	PCC	2.27	PCC
Yokota	13/36	2.61	PCC	1.95	PCC	1.91	PCC	1.94	PCC
Reese	17C/35C	2.37	AC	2.59	AC	2.15	AC	2.06	AC
Williams	12L/30R	2.52	PCC/AC	1.57	AC	1.68	AC	1.65	AC
<sup>c</sup> Williams	12C/30C	2.39	PCC	----	----	----	----	----	----
Williams	12R/30L	2.36	PCC	2.16	PCC	2.22	PCC	2.03	PCC
Laughlin	13L/31L	2.15	PCC/AC	2.31	PCC/AC	1.35	AC	----	AC
Elmendorf	15/33	2.21	AC	1.86	AC	2.05	AC/PCC	----	AC
Laughlin	13R/31L	1.87	AC	2.20	AC	1.56	AC	----	AC
Randolph	14R/32L	2.13	PCC/AC	1.90	PCC	1.48	FCC/AC	1.39	PCC/AC
<sup>d</sup> Vandenberg	12/30	1.59	AC	1.54	AC	1.60	AC	1.32	AC
Reese	17L/35R	----	PCC/AC	----	PCC/AC	1.39	AC	----	AC

<sup>a</sup>Av. rage DBV SDR 3 minutes after wetting.

<sup>b</sup>Asphalt emulsion diluted with water applied to asphaltic concrete.

<sup>c</sup>Runway under construction.

<sup>d</sup>New runway surface.

ORIGINAL PAGE IS  
 OF POOR QUALITY

TABLE 15.- DBV SDR OBTAINED AT 10 CIVIL AIRPORTS

EVALUATED NOVEMBER 1971 TO APRIL 1972 BY FAA  
 [From reference 29]

Airport	Runway	Touchdown area, rubber deposits				Trafficked, no rubber (wheel path)	
		SDR (a)	Surface	SDR (a)	Surface	SDR (a)	Surface
St. Louis Int.	12R/30L	4.79	12R:AC	3.51	30L:AC	2.90	AC
	6/24	2.48	24:PCC	2.13	6:PCC	1.85	PCC
	12L/30R	1.93	30R:PCC	1.35	12L:WCPCC	1.81	PCC
	17/35	1.77	17:PCC	1.63	35:PCC	1.79	PCC
Miami Int.	9R/27L	4.44	9R:AC	2.88	27L:AC	1.81	AC
	9L/27R	2.88	9L:AC	1.98	27R:AC	1.72	AC
	12/30	2.01	12:AC	1.75	30:AC	1.56	AC
	17/35	1.35	17:AC	1.32	35:AC	1.33	AC
Memphis Int.	17L/35R	3.82	17:PCC	3.51	35R:PCC	2.44	PCC
	9/27	1.83	27:AC	1.58	9:AC	1.32	AC
	17R/35L	---	---	---	---	1.47	PCC
	3/21	1.18	3:AC	1.16	21:AC	1.17	AC
New Orleans Int.	16/28	3.76	10:PCC	2.22	28:AC	2.26	PCC
	1/19	3.22	19:PCC	3.03	1:AC	2.17	PCC
	5/23	1.22	23:AC	---	5:AC	1.32	AC
Atlanta W. B. Hartsfield	9L/27R	2.88	9L:WCPCC	2.26	27R:WCPCC	1.38	WCPCC
	15/33	2.21	33:AC	1.72	15:AC	1.50	AC
	9R/27L	2.09	27L:GPCC	1.24	9R:GPCC	1.12	GPCC
	3/21	1.69	21:AC	1.52	3:AC	1.36	AC
Jacksonville Int.	7/25	2.77	7:PCC	2.53	25:PCC	2.12	PCC
	13/31	2.65	31:PCC	2.33	13:PCC	1.97	PCC
Greater Cincinnati	18/36	2.45	36:AC	1.93	18:AC	1.73	AC
	9R/27L	2.38	27L:AC	2.09	9R:AC	1.77	AC
	9L/27R	1.30	9L:PCC	1.15	27R:PCC	1.25	PCC
Charlotte Douglas	18/36	2.32	36:AC	1.39	18:AC	1.46	AC
	5/23	1.81	5:AC	1.38	23:AC	1.22	AC
Nashville Int.	13/31	2.12	31:AC	1.71	13:AC	1.69	AC
	2L/20R	2.08	20R:GAC	1.82	2L:GAC	2.04	GAC
	2R/20L	1.30	20L:AC	---	2R:AC	1.24	AC
Charleston Kanawha	5/23	1.33	23:GPCC	1.10	5:GPCC	1.09	GPCC
	14/32	1.20	32:AC	1.09	14:AC	1.16	AC

\*Average DBV SDR.

<sup>b</sup>New surface; under construction.

TABLE 16.- DBV AND AIRCRAFT SDR OBTAINED ON TRANSVERSE GROOVED RUNWAY SURFACES WITH AND WITHOUT RUBBER CONTAMINATION

[From reference 39]

Airport	Date tested	Runway	Rubber deposits	SDR		Surface; date installed	Groove pattern; date installed	Source
				DBV	Aircraft			
Cannon AFB	11/73	3/21	Heavy None	<sup>a</sup> 3.59 to 2.46 1.74	—	305 m (1000 ft) PCC, 2430 m (8000 ft) GPCC, 305 m (1000 ft) PCC; date unknown	51 x 6 x 6 mm (2 x 1/4 x 1/4 in.), groove 610 mm (2 ft) skip 610 mm (2 ft); 1973	Reference 8
Chaw AFB	7/74	4L/27R	Med-lt None	2.77 to 1.97 1.79	—	305 m (1000 ft) PCC, 1367 m (3500 ft) GPCC, 1370 m (4500 ft) GAC, 305 m (1000 ft) PCC; date unknown	51 x 6 x 6 mm (2 x 1/4 x 1/4 in.), groove 610 mm (2 ft) skip 610 mm (2 ft); 1971	Reference 8
Vance AFB	12/73	17R/35L	Lt-med None	<sup>a</sup> 2.50 <sup>a</sup> 1.50	—	457 m (1500 ft) PCC, 853 m (2800 ft) GPCC, 1036 m (3400 ft) AC; date unknown	51 x 6 x 6 mm (2 x 1/4 x 1/4 in.); 1973	Reference 8
Houston Int.	<sup>b</sup> 6/70	8L/26R	Heavy-med	3.46 to 2.94	—	PCC; date unknown	Ungrooved	Unpublished
	10/71		Lt-none	2.00 to 2.52	<sup>c</sup> 1.91 to 2.52		Ungrooved	
	2/25/71		None Heavy	1.13 to 1.44 2.27 to 2.43	<sup>d</sup> 1.10 to 1.50 —		51 x 6 x 6 mm (2 x 1/4 x 1/4 in.); 2/25/71	Unpublished
Miami Int.	3/73	9R/27L	Heavy None	4.62 to 3.51 2.43	—	AC overlay; 11/72	Ungrooved	Unpublished
		9L/27R	Heavy-med	3.16 to 2.38	—			
	5/73	9R/27L	Heavy-lt	2.42 to 1.51	—		38 x 10 x 6 mm (1 1/2 x 1/4 x 1/4 in.); <sup>e</sup> 1973	Unpublished
		9R/27L 9L/27R	None None	1.51 1.22	— —			
John F. Kennedy	7/69	1R/22L	None Heavy	1.75 2.20	<sup>f</sup> 1.57 1.86	PCC; 1959	38 x 10-5 x 3 mm (1 3/8 x 3/8-3/16 x 1/8 in.); 1967	Reference 1
	10/71		Lt-none	1.47 to 1.80	<sup>c</sup> 1.50 to 1.67			Unpublished
Atlanta Int.	11/71	9R/27L	Heavy-med None	2.09 to 1.24 1.12	—	PCC; date unknown	32 x 10-3 x 6 mm (1 1/4 x 3/8-1/8 x 1/4 in.); 1967	Reference 10
Nashville Int.	4/72	2L/20R	Lt None	2.08 to 1.82 2.04	—	AC; date unknown	32 x 6 x 6 mm (1 1/4 x 1/4 x 1/4 in.); 1970	Reference 10
Harry S. Truman	6/70	9/27	Heavy None Heavy None	2.28 1.40 1.69 1.18	— —	AC; date unknown	Ungrooved 38 x 6 x 6 mm (1 1/2 x 1/4 x 1/4 in.); 4/70	Unpublished
Wright-Patterson AFB	7/69	8/26	None Heavy-lt	1.35 1.50	<sup>f</sup> 1.38 1.47	PCC, 1960	51 x 6 x 6 mm (2 1/4 x 1/4 x 1/4 in.), groove 610 mm (2 ft) skip 610 mm (2 ft); 1968	Reference 1

<sup>a</sup>DBV test area contained both grooved and ungrooved pavements.

<sup>b</sup>Rubber removed after test.

<sup>c</sup>B-727.

<sup>d</sup>DC-9.

<sup>e</sup>9L/27R being grooved at time of test.

<sup>f</sup>C-141.

ORIGINAL PAGE IS  
OF POOR QUALITY

TABLE 17.- DEW SDR AND NASA GREASE TEST ATD OBTAINED ON RUNWAYS EVALUATED BY THE FAA TRIAL APPLICATION -  
 RUNWAY FRICTION CALIBRATION AND PILOT INFORMATION PROGRAM DURING AUGUST AND SEPTEMBER 1975

Airport	Runway	Surface (a)		Touchdown area, rubber deposits			Trafficked, no rubber		
				DEW SDR	ATD		DEW SDR	ATD	
					mm	in.		mm	in.
Allentown	13	GAC	1.0	1.07	1.56	0.061	1.08	1.48	0.058
	31		1.29	1.49	.059	1.08	1.48	.058	
	6	GAC	0.75	2.07	1.52	.060	1.66	1.48	.055
	24		1.71	1.60	.063	1.66	1.46	.052	
Akron-Canton	1	AC	1.4	2.71	0.229	0.009	2.01	0.305	0.012
	19		2.19	.229	.009				
	5	AC	1.4	1.32	.254	.010	1.47	.330	.013
	23		1.26	.330	.013				
Boston Logan	4L	GAC	1.0	1.12	---	---	0.90	---	---
	22R		1.00	---	---	.90	---	---	
	4R	GAC	1.0	1.62	---	---	1.96	---	---
	22L		1.75	---	---	1.96	---	---	
	15R	GAC	1.0	1.39	---	---	2.00	---	---
33L	2.50		---	---	2.00	---	---		
Buffalo	5	AC	1.0	2.06	0.838	0.033	2.30	0.864	0.034
	23		2.68	1.092	.043	2.30	.864	.034	
	b <sub>14</sub>								
	b <sub>32</sub>								
Burlington	15	AC	1.0	2.09	0.559	0.022	1.75	0.584	0.023
	33		2.04	.598	.026				
Charleston, W. Va.	5	GPCC	0.8	1.27	0.211	0.008	1.35	0.221	0.009
	23		1.42	.165	.007				
	b <sub>14</sub>								
	b <sub>32</sub>								
Cincinnati	18	GAC	1.5	1.51	1.346	0.053	2.05	1.016	0.040
	36		1.70	1.270	.050				
	9R	GPCC	1.5	1.34	.838	.033	1.38	1.194	0.047
	27L		1.78	1.270	.050				
Cleveland	5R	GAC	1.3	1.7	0.737	0.029	2.14	1.092	0.043
	23L		2.4	.279	.011				
	10L	GAC	0.8	1.30	1.118	.044	1.57	1.702	.067
	28R		1.39	.717	.029				
Detroit	3L	GPCC	1.0	1.58	1.270	0.050	1.68	1.270	0.050
	21R		1.65	1.270	.050				
	9	PCC/AC	1.0	2.10	.432	.017	1.91	.508	.020
	27		2.77	.076	.003				
Dulles	1L	PCC	1.0	3.11	0.152	0.006	2.98	0.254	0.019
	19R		3.90	.102	.004				
	1R	PCC	1.0	4.48	.229	.009	3.13	.254	.010
	19L		3.12	.229	.011				
Ft. Wayne	4	PCC/AC	0.9	2.00	0.330	0.013	1.55	0.533	0.021
	22		2.05	.203	.008				
	9	PCC/AC	N/A	1.77	1.016	.040	1.80	.508	.020
	27		1.81	.559	.022				
Grand Rapids	8R	PCC/AC	1.5	2.36	0.254	0.010	1.57	0.127	0.005
	26L		1.96	.254	.010				
Madison	18	PCC	1.5	1.68	0.686	0.027	1.43	1.016	0.040
	36		1.35	1.118	.044				
	13	AC	1.5	1.62	.381	.015	1.54	.127	.005
	31		1.70	.254	.010				

<sup>a</sup>Number on right of column represents the runway transverse slope in percent.  
<sup>b</sup>Under construction.

TABLE 17.- Concluded

Airport	Runway	Surface (a)		Touchdown area, rubber deposits			Trafficked, no rubber		
				DBV SDR	ATD		DBV SDR	ATD	
					mm	in.		mm	in.
Milwaukee	<sup>b</sup> 1L								
	<sup>b</sup> 19R								
	7R 25L	PCC	1.0	1.67 3.02	0.838 1.118	0.033 .044	1.56	0.432	0.017
Moline	9	AC	1.0	2.34	0.508	0.020	2.65	0.506	0.020
	27			2.77	.102	.004			
	12 30	P.C	1.0	2.66 2.91	.216 .152	.009 .006	2.49	.127	.005
Peoria	30	GAC	1.25	1.36	0.965	0.038	1.16	1.397	0.055
	12			1.52	.991	.039			
	4 22	AC	1.0	1.14 1.44	.635 .305	.025 .012	1.43	1.270	.050
Philadelphia	9R	AC	1.0	4.99	0.127	0.005	2.47	0.279	0.011
	27L			3.57	.127	.005			
Pittsburg	10R	GAC	1.0	2.15	1.549	0.061	1.63	1.600	0.063
	28L			2.54	1.549	.061			
	10L	GAC	1.5	1.43	1.549	.061	1.35	1.600	.063
	28R			1.49	1.626	.064			
Portland, Maine	11	AC	1.0	1.54	0.737	0.029	1.27	0.737	0.029
	29			1.41	.762	.030			
	18 35	AC	1.0	1.86 1.83	.254 .279	.010 .011	1.77	.279	.011
Rochester, N.Y.	10	AC	1.0	1.74	0.559	0.022	1.79	0.356	0.014
	28			2.18	.178	.007			
	4 22	PCC	1.0	3.68 4.50	.102 .127	.004 .005	3.60	.152	.006

<sup>a</sup>Number on right of column represents the runway transverse slope in percent.

<sup>b</sup>Under construction.

TABLE 18.- U.S. POROUS ASPHALT RUNWAY SURFACE CONSTRUCTION

Year	Airport	Runway	Year	Airport	Runway	
1970	Hahn AB - M	11/29	1973	St. Louis Lambert - C	6/24	
	RAF Mildenhall - M	1/29		1974	Aberdeen (S. Dak.) - C	13/31
	Wiesbaden AB - M	8/26			Farmington (N. Mex.) - C	7/25
1971	Dallas NAS - M	17/35	Greensboro-High Point - C		14/32	
	Gallup (N. Mex.) - C	6/24	Hill AFB - M		14/32	
1972	Denver Stapleton - C	8L/26R	Las Vegas (Nev.) - C		7/25	
	Denver Stapleton - C	8R/26L	RAF Bentwaters - M		7/25	
	Great Falls Int. - C	16/34	RAF Lakerheath - M		6/24	
	Hot Springs (Va.) - C	6/24	Roswell (N. Mex.) - C		17/35	
	Nashville Metro. - C	2L/20R	Sioux City (Idaho) - C		17/35	
	Sioux Falls (N. Dak.) - C	15/33	1975		Boise (Idaho) - C	10R/28L
	Springfield (Mo.) - C	13/31		Jackson Hole (Wyo.) - C	18/36	
	Vernal (Utah) - C	16/34		Jamestown (N. Dak.) - C	12/30	
Wichita Mun. - C	N/A	Las Vegas (Nev.) - C		1R/19L		
1973	Bellingham (Wash.) - C	16/34		Missoula (Mont.) - C	11/29	
	Cedar City (Utah) - C	2/20	Monroe (La.) - C	4/22		
	Pease AFB - M	16/34	Pierre (S. Dak.) - C	13/31		
	Portland (Maine) - C	11/29				
	RAF Alconbury - M	12/30				
	Rapid City (S. Dak.) - C	14/32				
	Ramstein AB - M	9/27				
	Salt Lake City (Utah) - C	16L/34R				
Salt Lake City (Utah) - C	16R/34L					

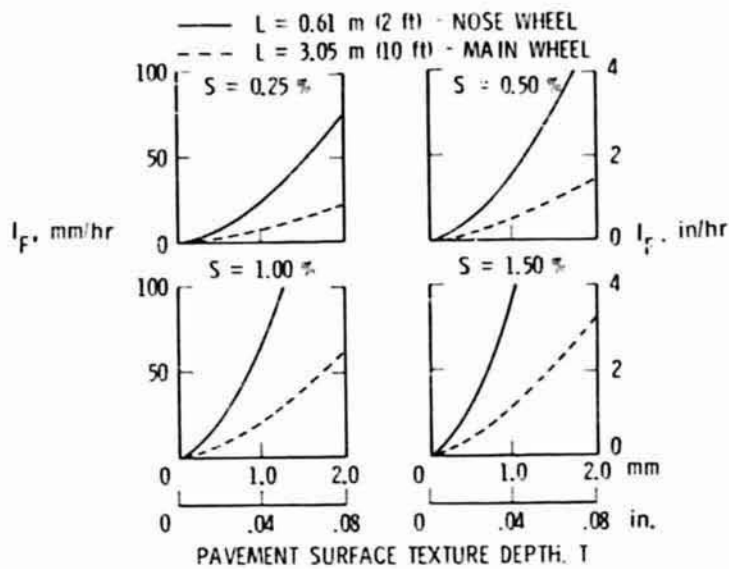


Figure 1.- Rainfall rate required to flood tire path on conventional runway surfaces. Landings on center line.

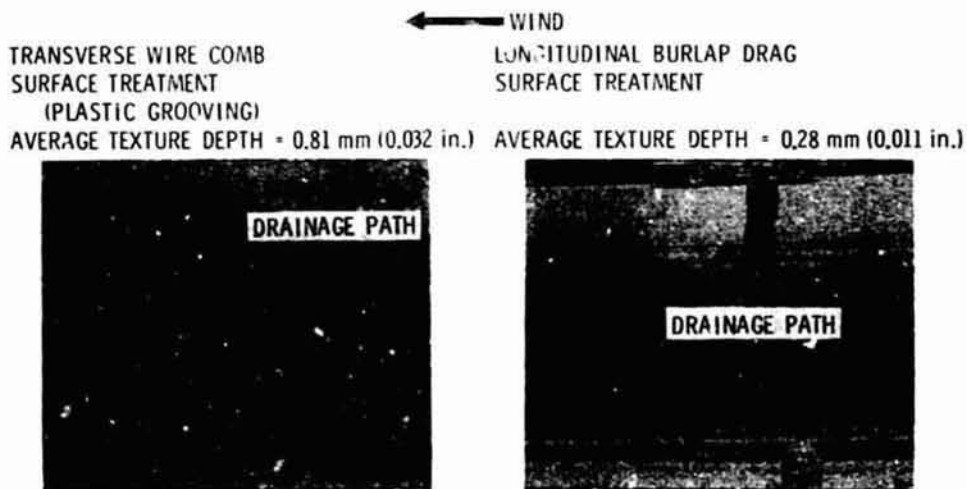


Figure 2.- Water drainage from concrete runway at PHF. Water truck wetting; runway 6/24; wind from 60° at 10 knots.



Figure 3.- Space shuttle landing facility at KSC.

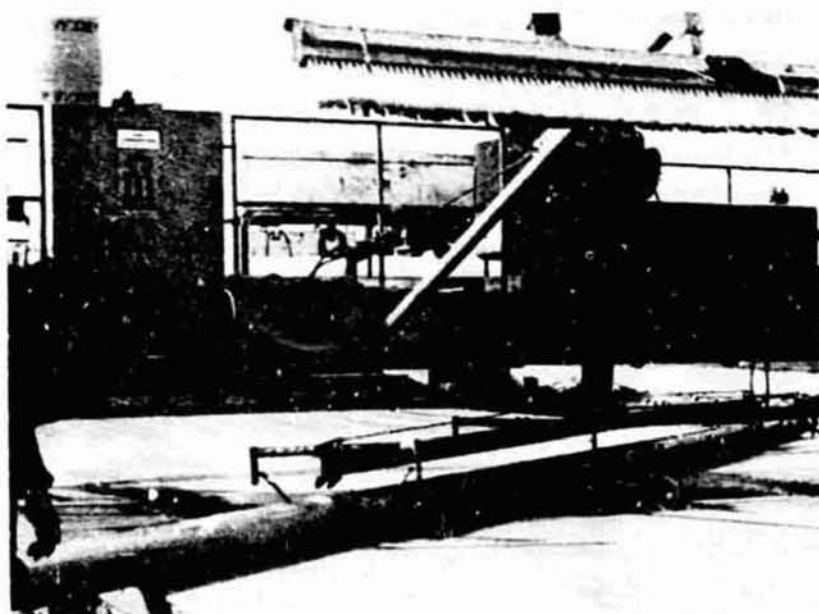


Figure 4.- Space shuttle landing facility at KSC with slip-form paving equipment, leveling tube, and longitudinal broom.

ORIGINAL PAGE IS  
OF POOR QUALITY



Figure 5.- Space shuttle landing facility at KSC with pavement grooving machine (diamond blades).



LONGITUDINAL BROOM FINISH  
 ATD = 0.38 to 0.64 mm  
 (0.015 to 0.025 in.)

TRANVERSE GROOVE PATTERN  
 ATD = 1.70 to 1.91 mm  
 (0.067 to 0.075 in.)

Figure 6.- Concrete runway surface texture of space shuttle landing facility at KSC.

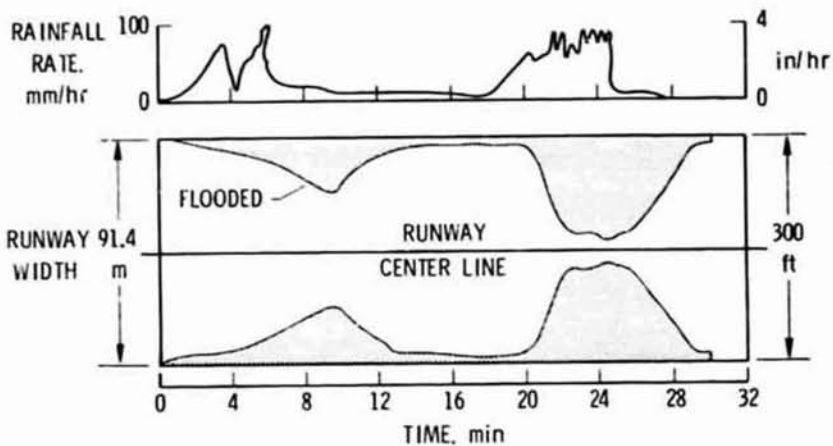


Figure 7.- Surface flooding on space shuttle grooved runway during thunderstorm 6/20/76.



Figure 8.- Water drainage from grooved and ungrooved asphalt. Grooving pattern,  $38 \times 6 \times 6$  mm ( $1\frac{1}{2} \times \frac{1}{4} \times \frac{1}{4}$  in.).

NASA TRACK TEST: DC-9 MLG RIB-TREAD TIRE  
 WATER DEPTH: 2.5 TO 3.8 mm (0.10 TO 0.15 in.)  
 TIRE INFLATION PRESSURE: 965 kPa (140 lb/in<sup>2</sup>)  
 $(V_P)_{\text{spin-down}} = 106 \text{ knots}$   
 $(V_P)_{\text{spin-up}} = 91 \text{ knots}$

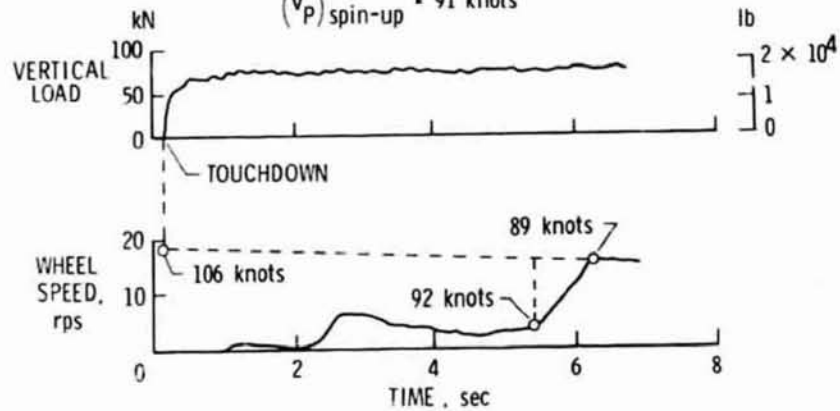


Figure 9.- Delayed wheel spin-up at touchdown on flooded runway.



Figure 10.- B-737 tire reverted rubber skid patch after 1.8 km (6000 ft) locked-wheel skid on wet smooth concrete.

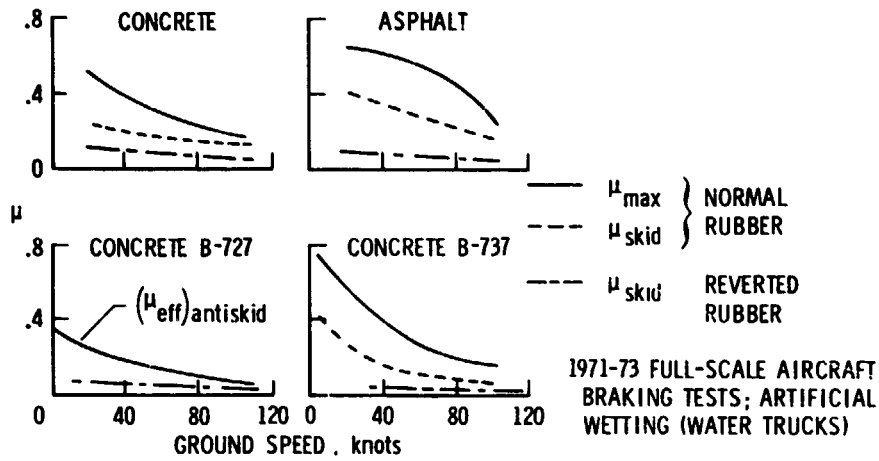


Figure 11.- Aircraft flight test confirmation of reverted rubber hydroplaning 1965 NASA track; 32 x 8.8 aircraft tire; flooded runway.

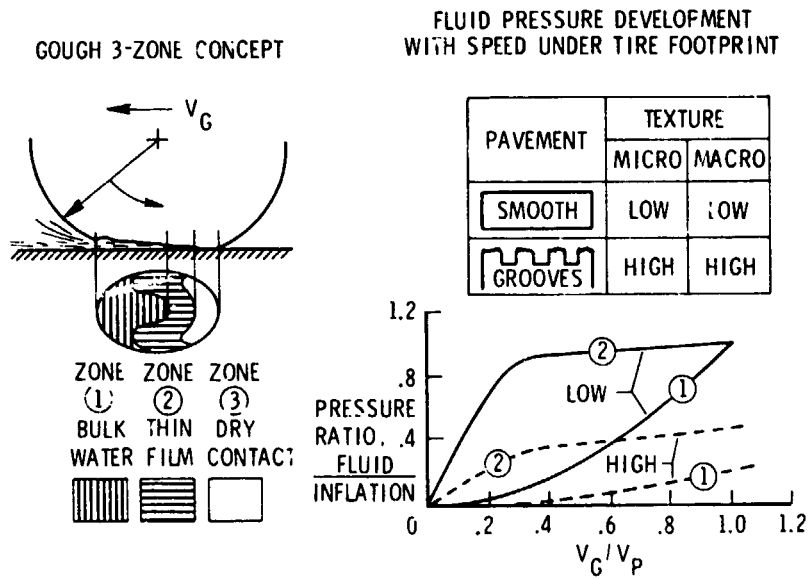


Figure 12.- NASA model for combined viscous and dynamic tire hydroplaning.

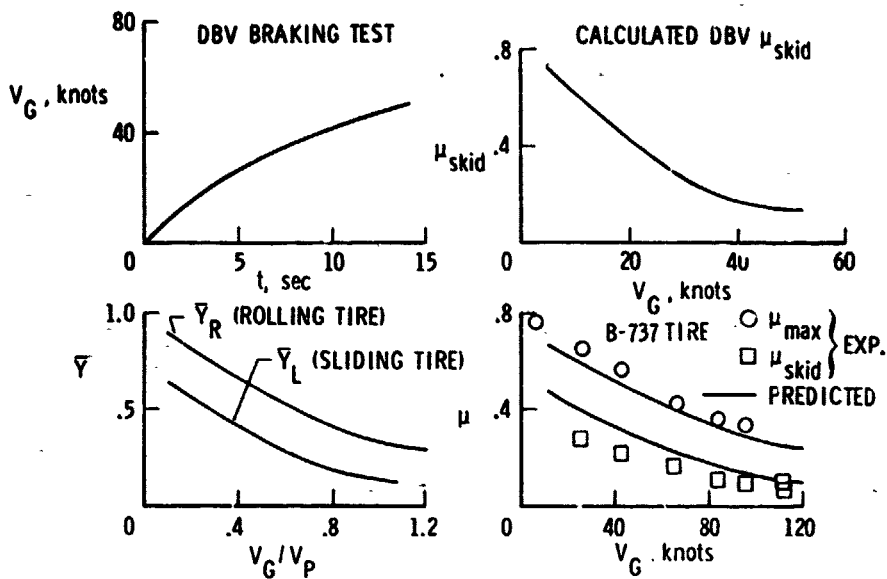


Figure 13.- Prediction of aircraft tire friction coefficient from ground-vehicle braking test on a wet runway by NASA theory.

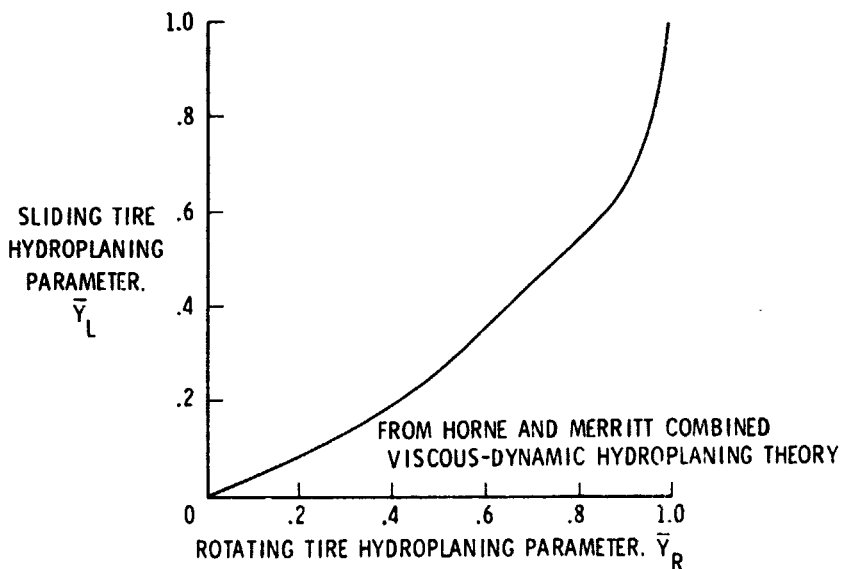


Figure 14.- Empirically derived relationship between sliding ( $\bar{Y}_L$ ) and rotating ( $\bar{Y}_R$ ) tire hydroplaning parameters.

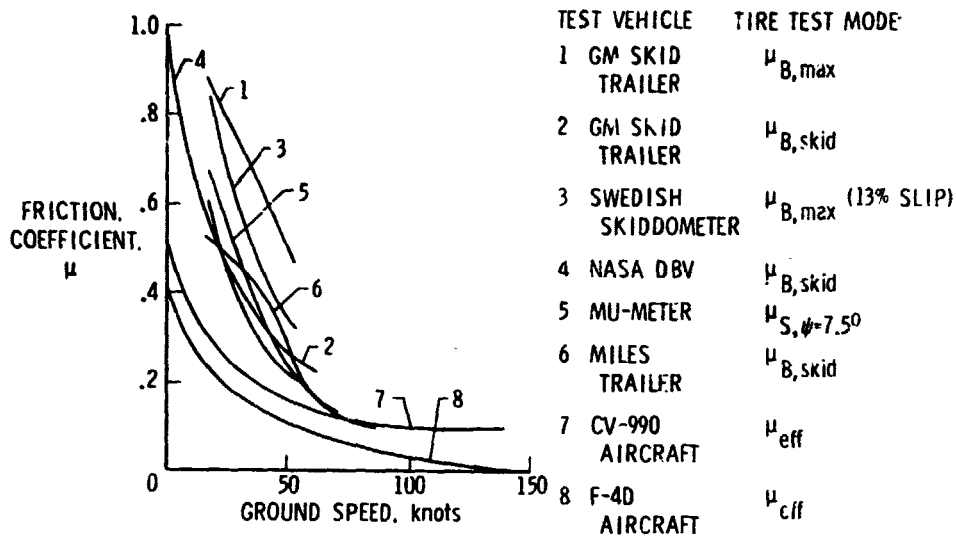


Figure 15.- Aircraft/ground-vehicle correlation problem for wet and puddled smooth concrete surface.

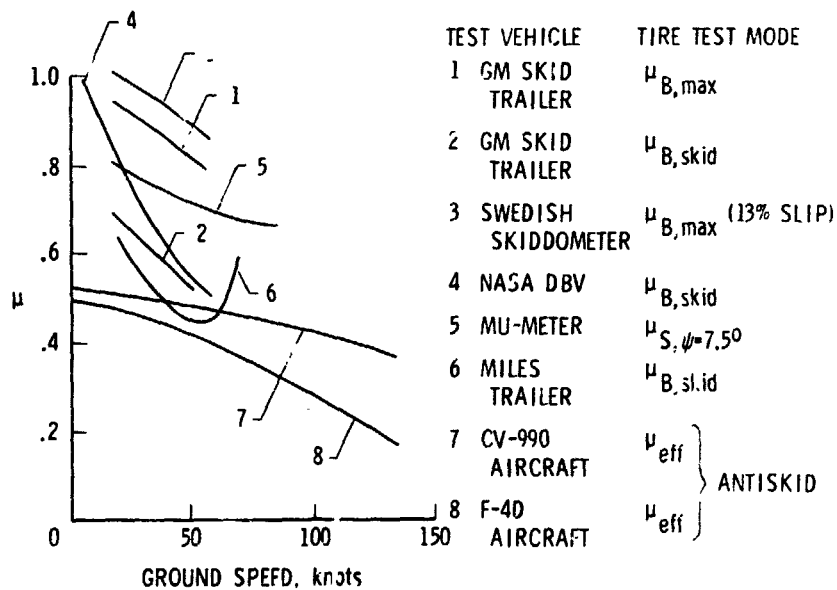


Figure 16.- Aircraft/ground-vehicle correlation problem for wet and puddled grooved asphalt.

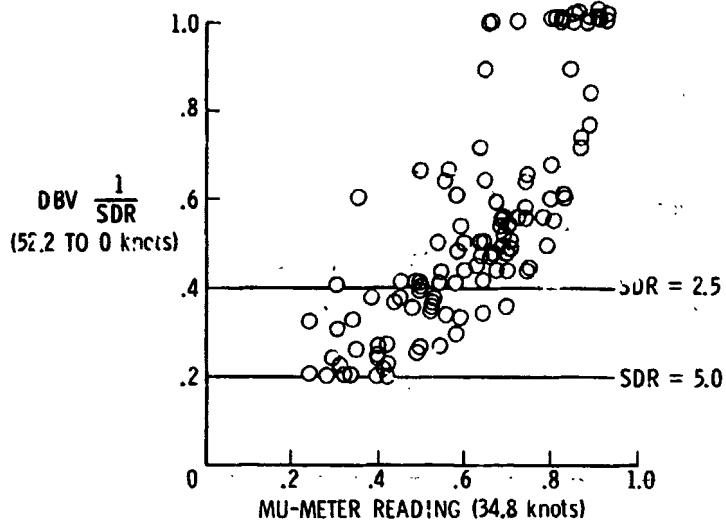


Figure 17.- DBV/Mu-Meter relationship found by USAF tests (ref. 28).

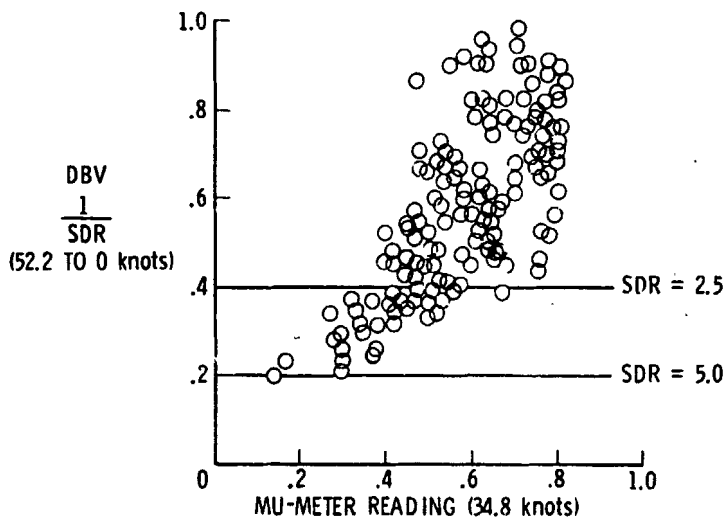


Figure 18.- DBV/Mu-Meter relationship found by FAA tests on 31 runways.

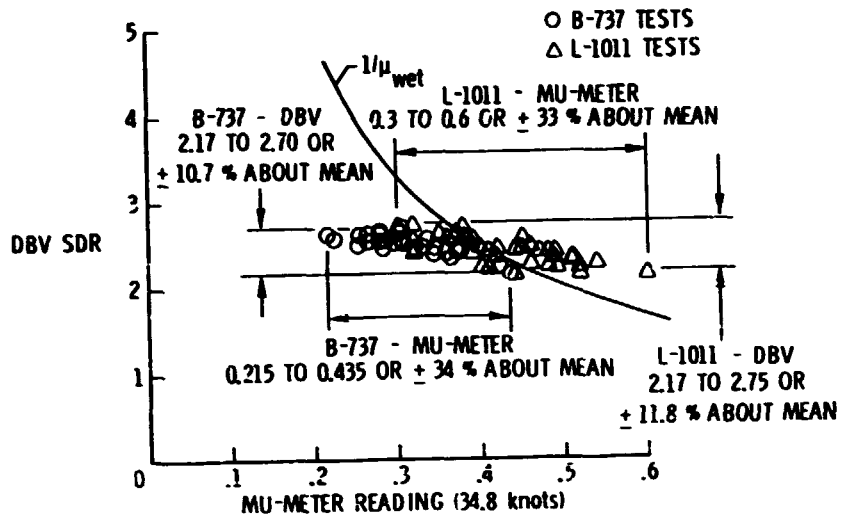


Figure 19.- Comparison of NASA DBV with Mu-Meter.

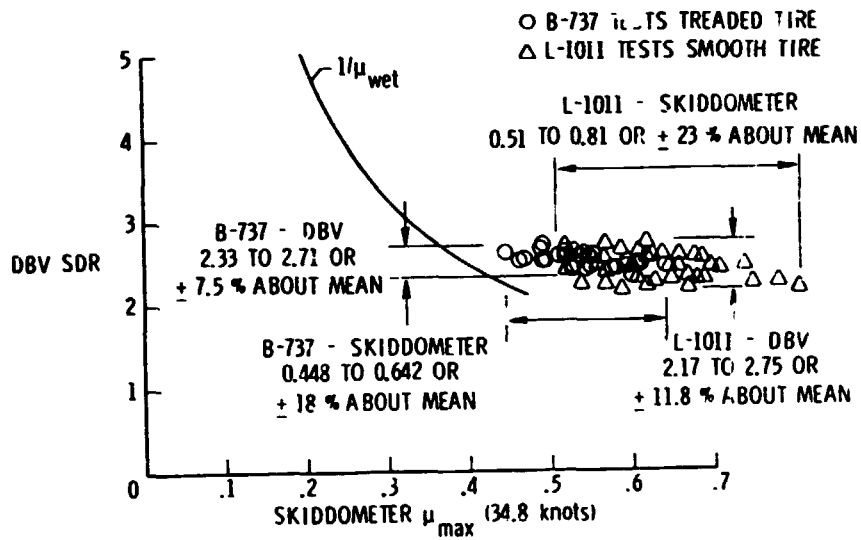


Figure 20.- Comparison of NASA DBV with skiddometer.

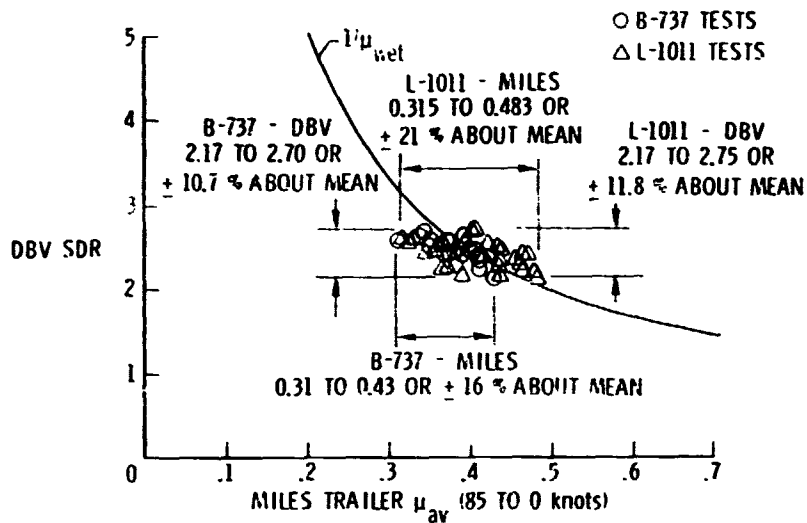


Figure 21.- Comparison of NASA DBV with Miles trailer.

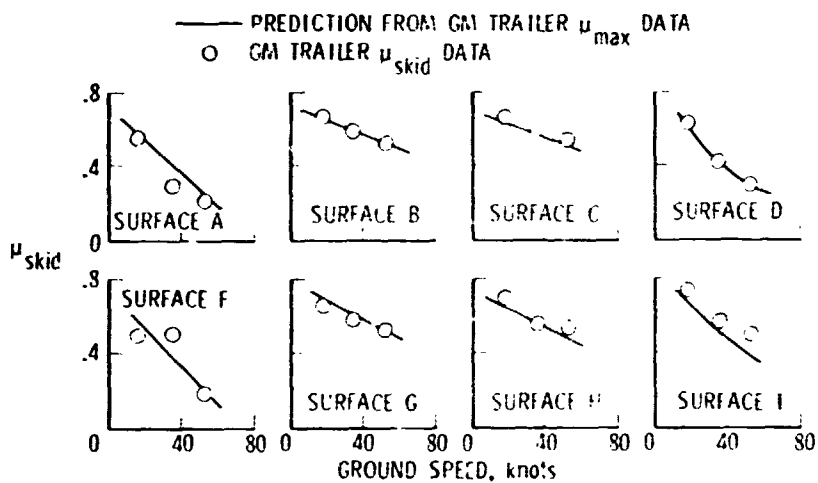


Figure 22.- Prediction of GM trailer  $\mu_{skid}$  from GM trailer  $\mu_{max}$  data. ASTM smooth tread tire; data from reference 22.

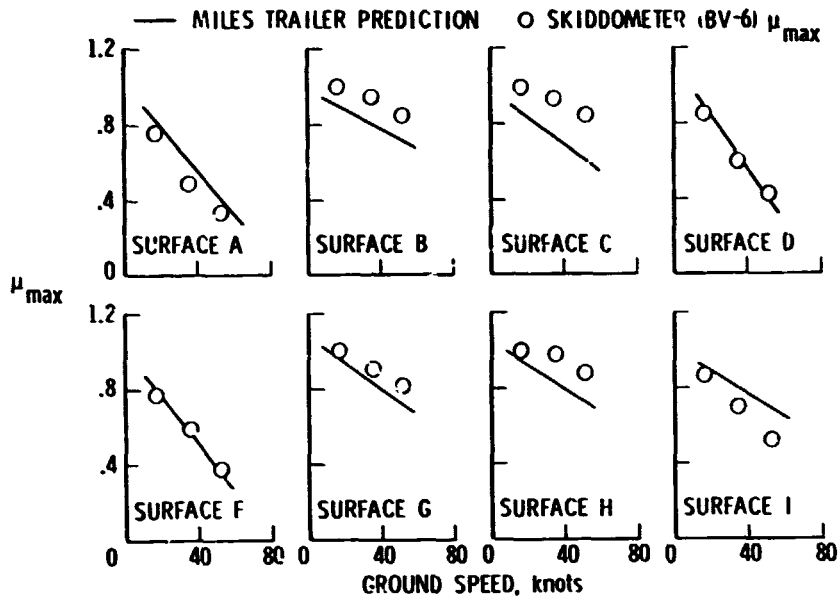


Figure 23.- Prediction of skiddometer  $\mu_{\max}$  from Miles trailer  $\mu_{\text{skid}}$  data. Data from references 21 and 22.

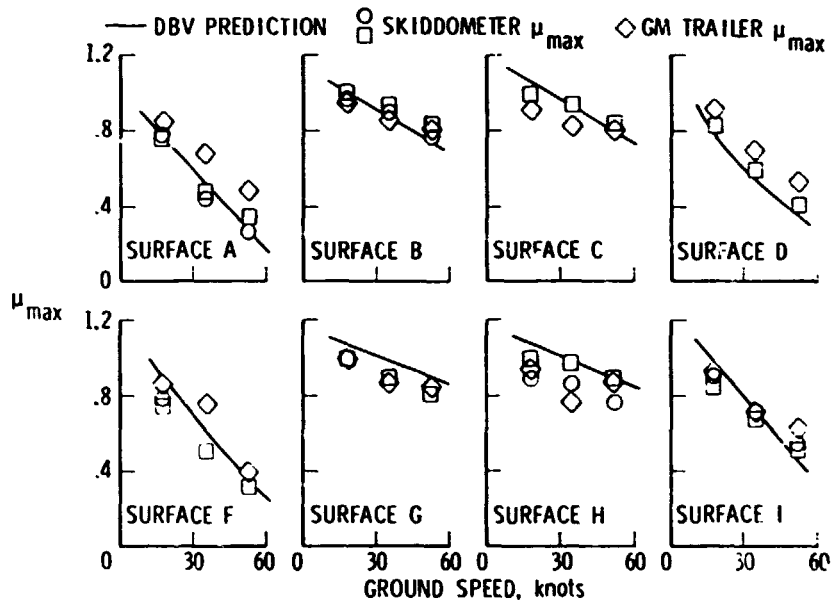


Figure 24.- Prediction of skiddometer and GM trailer  $\mu_{\max}$  from DBV  $\mu_{\text{skid}}$  data. Data from references 21, 22, and 30.

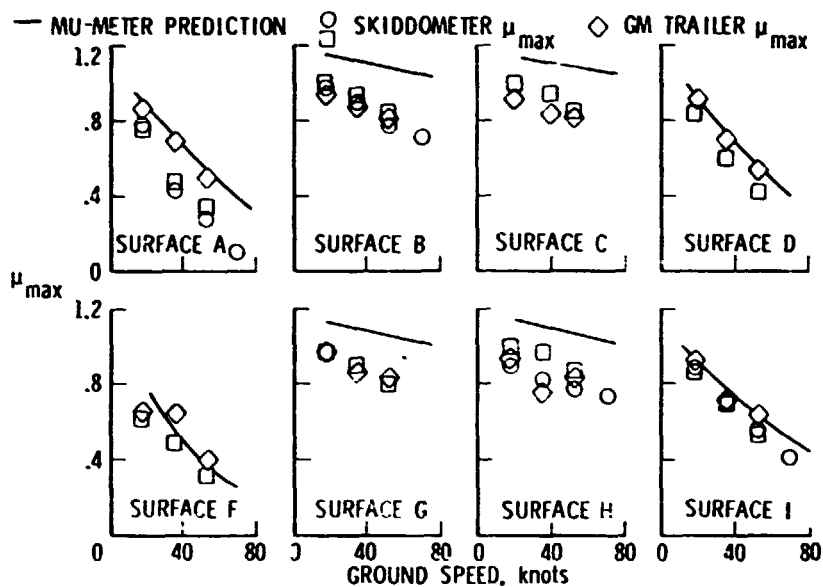


Figure 25.- Prediction of skiddometer and GM trailer  $\mu_{max}$  from Mu-Meter friction reading ( $\psi = 7.5^\circ$ ). Data from references 21, 22, and 30.

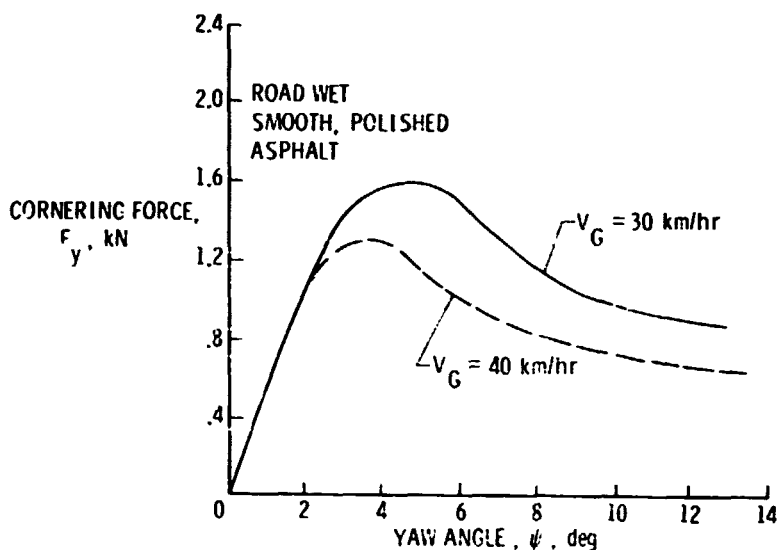


Figure 26.- Effect of ground speed on cornering-force-yaw-angle relationships for 5.60-13 automobile tire.  $F_z = 2.70$  kN;  $p = 167$  kPa; from reference 31.

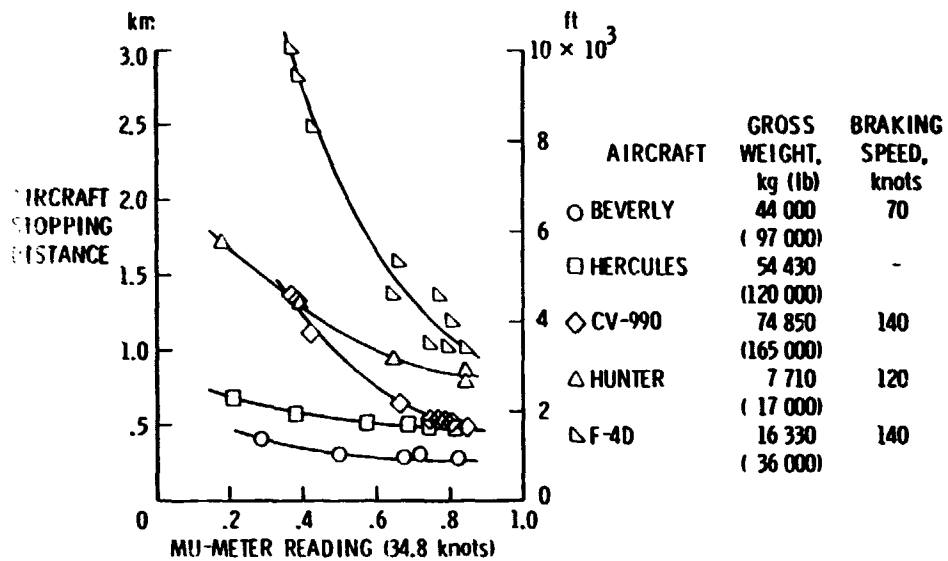


Figure 27.- Mu-Meter correlation with aircraft stopping distances on wet surfaces.

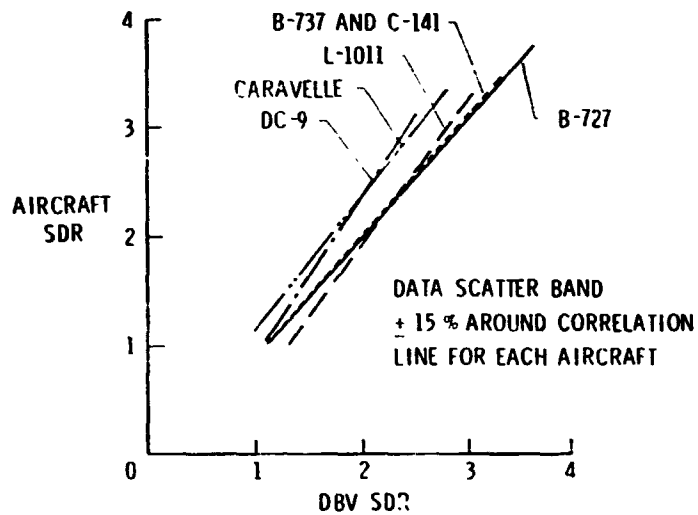


Figure 28.- Aircraft/DBV correlation on wet runways for different jet transports.

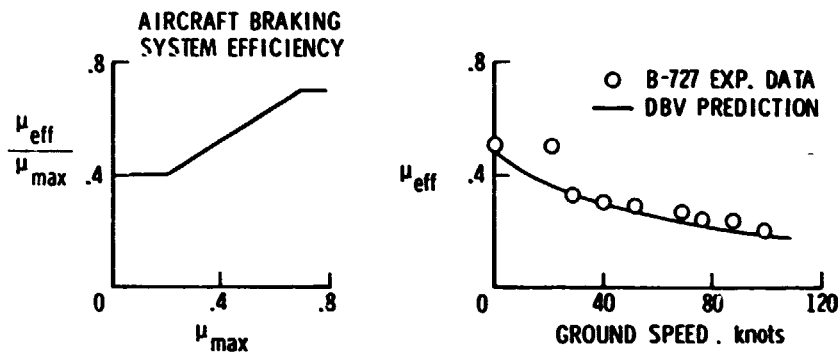


Figure 29.- Prediction of aircraft braking performance on wet runway from DBV braking test. JFK runway 4R/22L; grooved concrete; water truck wetting.

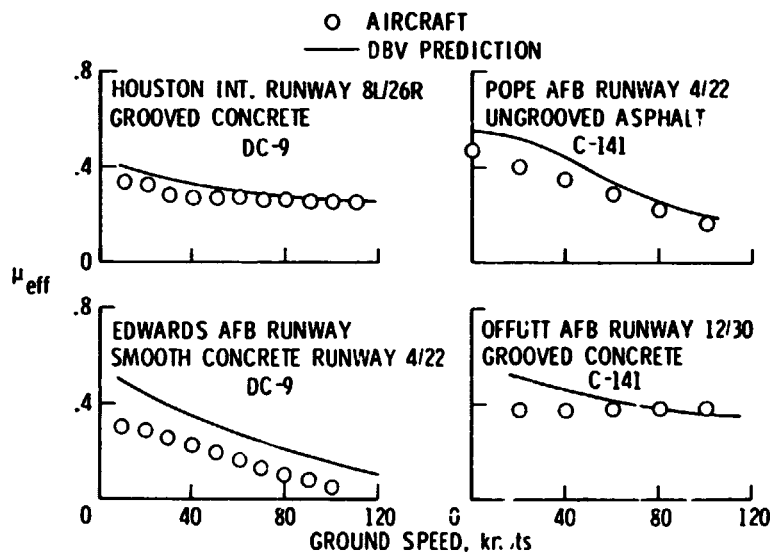


Figure 30.- Prediction of aircraft braking performance on wet runways from DBV braking test for DC-9 and C-141 jet transports.

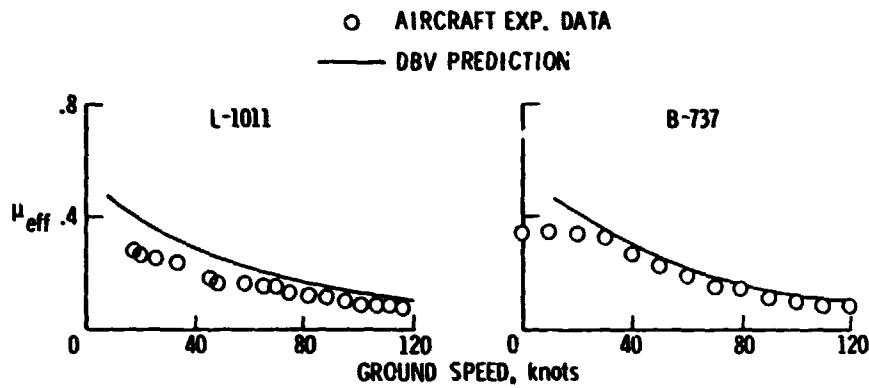


Figure 31.- Prediction of aircraft braking performance on wet runway from DBV braking test for B-737 and L-1011 jet transports. Roswell runway 3/21; smooth concrete.

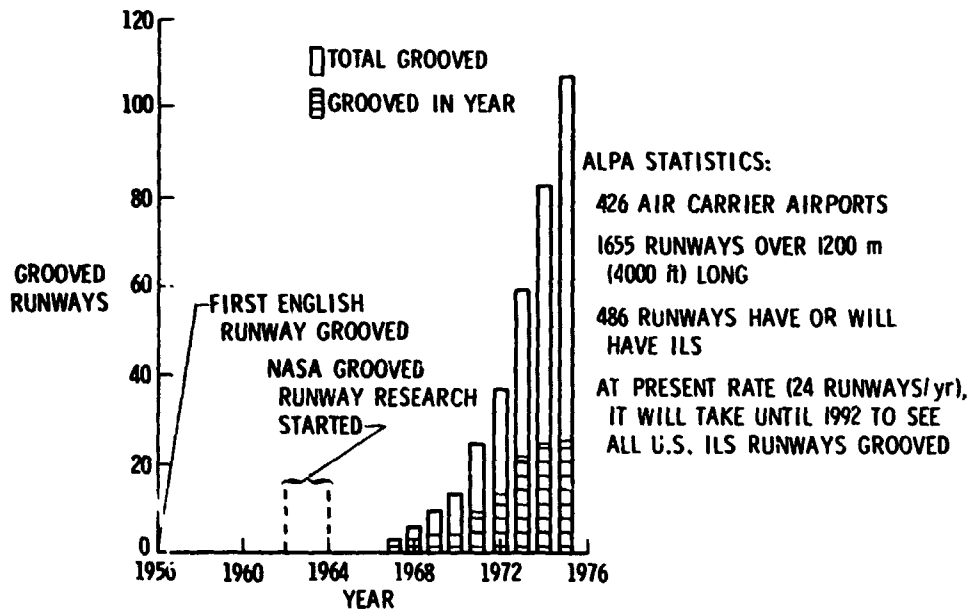


Figure 32.- Number of grooved runways at U.S. air carrier airports.



(a) Plastic grooving with segmented drum.



(b) Plastic grooving with wire comb.

Figure 33.- Examples of plastic grooving of Portland cement concrete.

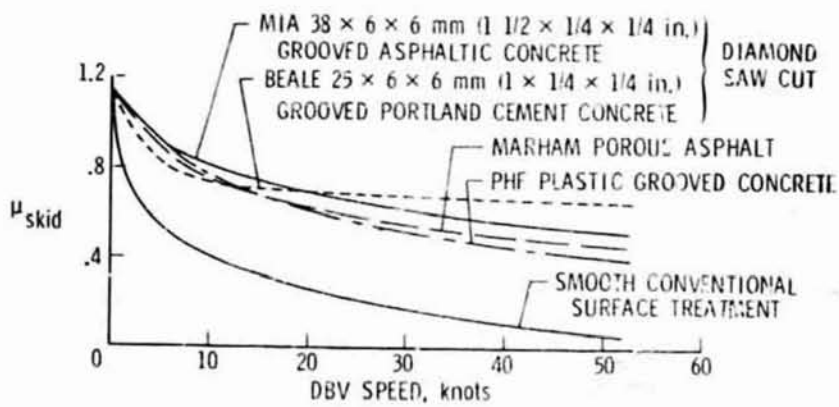


Figure 34.- Wet skid resistance of several new type runway surface treatments. Artificial wetting.

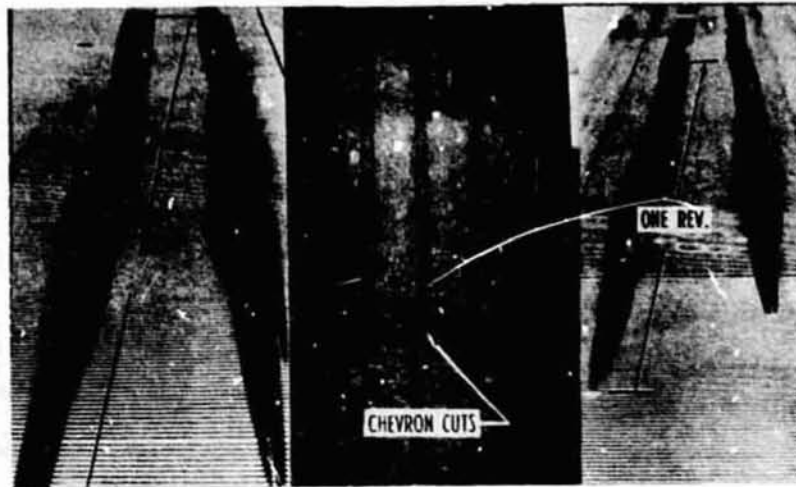


Figure 35.- Tire damage from wheel spin-up at touchdown on dry grooved runway. Wallops grooved concrete; groove pattern,  $25 \times 6 \times 6$  mm ( $1 \times 1/4 \times 1/4$  in.); CV-990 jet transport MLG tire, size  $41 \times 15.0-18$ ;  $p = 1102$  kPa ( $160$  lb/in<sup>2</sup>);  $V_G = 125$  knots.

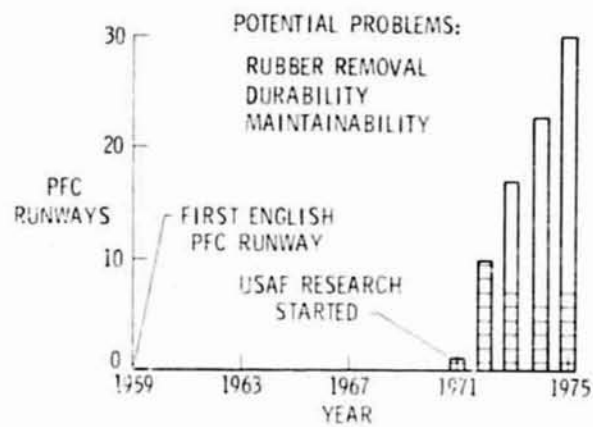


Figure 36.- Number of porous friction course runways at U.S. air carrier airports.

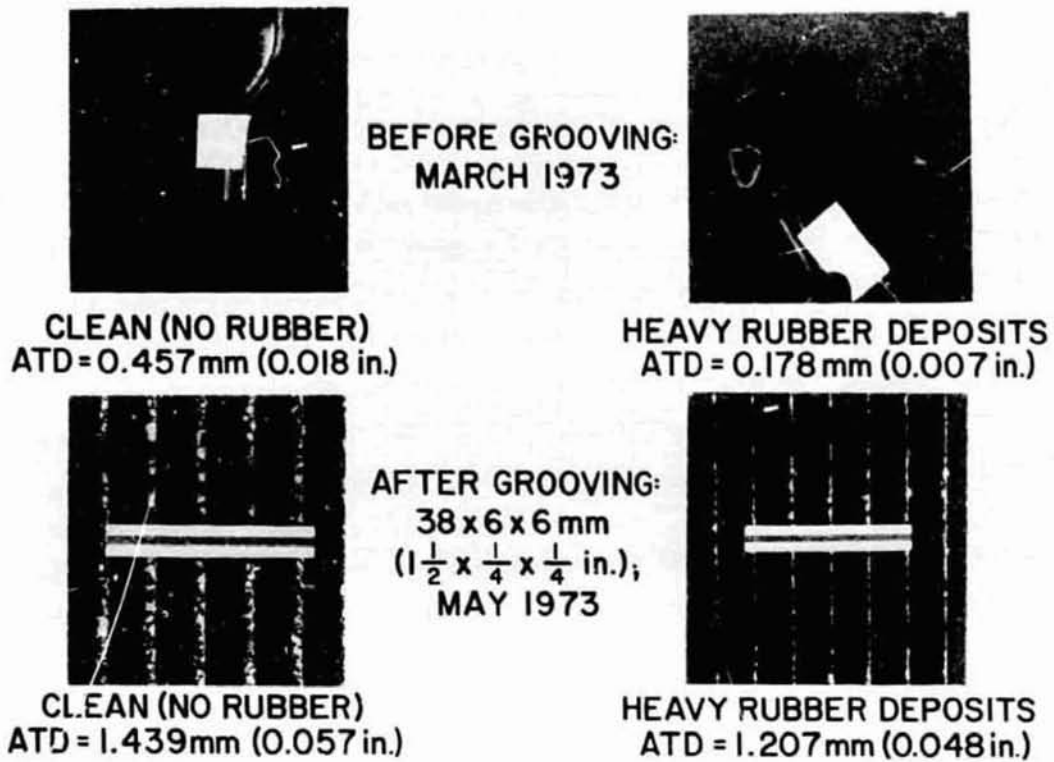


Figure 37.- Effect of rubber deposits on runway surface texture.

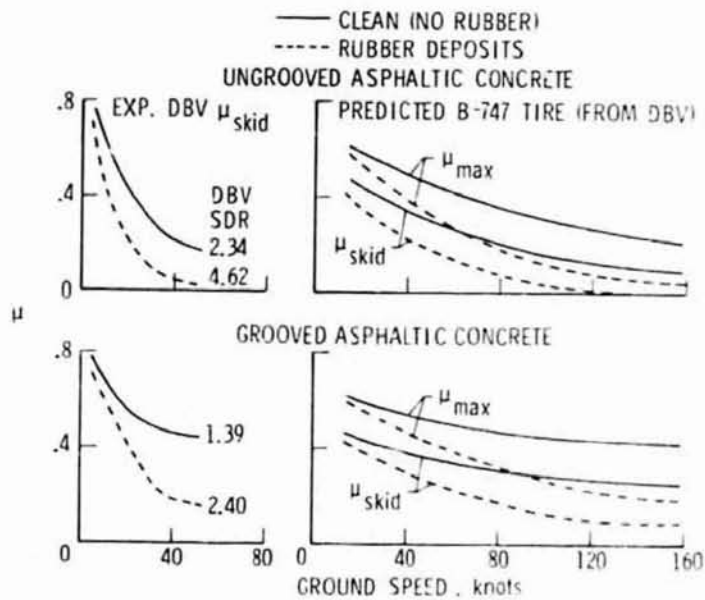


Figure 38.- Effect of rubber deposits on runway traction before and after grooving.



BEFORE RUBBER REMOVAL  
MAY 15, 1975



AFTER RUBBER REMOVAL  
MAY 30, 1975

Figure 39.- Approach end of LAFB runway 25 before and after rubber removal by high-pressure water blast.

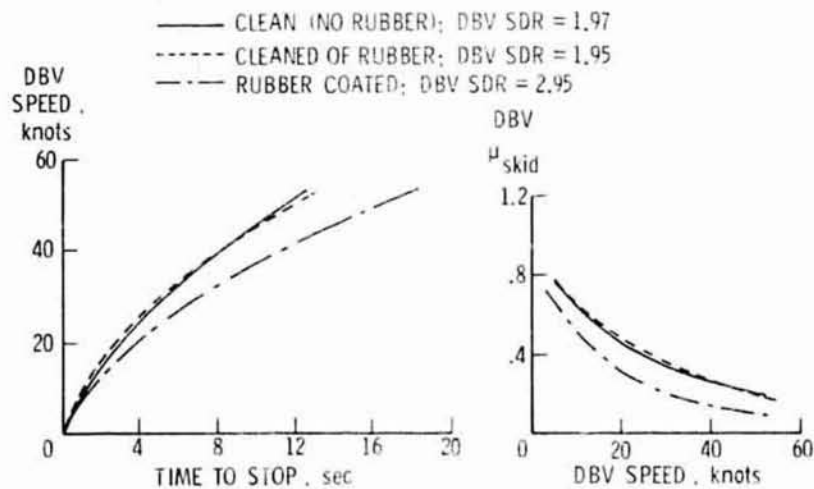


Figure 40.- Effect of rubber removal by high-pressure water blast on runway traction. LAFB runway 25; May 1975.